Preparation and Characterization of HA Powders - Dense and Porous HA Based Composite Materials

By

DENİZ ŞİMŞEK

A Dissertation Submitted to the
Graduate School in Partial Fulfillment of the
Requirements for the Degree of

MASTER OF SCIENCE

Department : Materials Science and Engineering
Major: Materials Science and Engineering

Izmir Institute of Technology
Izmir, Turkey

We approve the thesis of **Deniz ŞİMŞEK**

..... **07.10.2002**

Prof.Dr.Muhsin ÇİFTÇİOĞLU

Supervisor

Department of Chemical Engineering

..... **07.10.2002**

Prof.Dr. Şebnem HARSA

Co-Supervisor

Department of Food Engineering

..... **07.10.2002**

Assoc.Prof.Dr. Mustafa GÜDEN

Department of Mechanical Engineering

..... **07.10.2002**

Assist.Prof.Dr. Funda TIHMINLIOĞLU

Department of Chemical Engineering

..... **07.10.2002**

Prof.Dr.Muhsin ÇİFTÇİOĞLU

Head of Interdisiplinary

Materials Science and Engineering Program

ACKNOWLEDGEMENTS

I would like to thank and express my deepest gratitude to Professor Muhsin Çiftçioğlu for his supervision, guidance, support, understanding and encouragement during this study and in the preparation of this thesis. I also wish to offer my sincere thanks to Professor Şebnem Harsa for her guidance and support.

I also present my deepest thanks to Specialist Rukiye Çiftçioğlu for her kind supports, contributions and help in every step of this work.

I would like to thank to my love Hacer for her endless support, patience and encouragement.

Finally, I am very greatful to my family for their endless understanding and encouragment.

Verba Volant, Scripta Manent.

ABSTRACT

The synthesis of hydroxyapatite (HA) powders, whiskers and preparation of HA based ceramics have been investigated in this work. Commercial HA powders were used for comparion purposes. The powder and sintered ceramics were characterized by optical microscopy, SEM,XRD, particle size determination, dilatometry and mechanical testing.

Ca-P powders were synthesized by using $(NH_4)_2HPO_4$ and $Ca(NO_3)_2$. $4H_2O$ by a precipitation method in aqueous medium. Ca/P ratio was set to 1,5 and 1,667 that yield the mixture of Ca-P phases and HA powder respectively at pH 10, 60 ^oC and 24hrs aging. Ca/P ratio was set to 1,667 and the effect of pH of the medium, aging temperature and aging time on the powder characteristics was investigated. pH was set to 4,6,8,9,10 and 11 while aging temperature and time kept constant at 60 ^oC and 24 hrs. Formation of HA powder was observed over pH 8. Agglomerated Monetite-Brushite powder was obtained at pH=4. Monodispersed prismatic Brushite crystals were obtained at pH=6. Aging temperature investigation was performed at 30-90 ºC at pH=10 for 24 hrs aging. Increase in the aging temperature led to formation of more thermally stable HA phase. Precipitates were aged for 0, 0.5, 1, 24 and 48 hours at constant pH=10 and temperature 60 ºC. Thermally stable HA phase was obtained over 24hrs aging. All of the oven-dried precipitates were heat treated at 400-1250 ºC range in order to investigate the thermal stability and phase structure development. Optimum conditions for the precipitation of thermally stable HA powder was determined as pH=10, 60 ^oC aging temperature and 24 hrs aging time that yields equaxed HA powder with particle size about 40-60 nm.

Molten salt synthesis (MSS) and hydrothermal synthesis (HDT) were used to prepare HA whiskers. XRD patterns of both whiskers have shown that HA was the dominant phase in whiskers and no other phases were detected. Hydrothermal whiskers had submicron diameters with an average aspect ratio of 20. The diameter of the MSS whiskers were in the 1-5 micron range and were mostly hexagonal with an average aspect ratio of 10.

10, 20 and 30 vol% whisker containing composites were prepared. Sintering behavior and mechanical properties were investigated. 98% TD of HA ceramics (3.16 g/cm^3) was obtained in the 1150-1250^{0}C range. 80-90% TD was obtained at above 1200^{0}C for the MSS whisker composites with very little shinkages. Densities of the

HDT whisker containing composites were higher than those of the MSS whisker composites. The highest hardness value was determined as 537 Hv for the HA ceramics 1250^{o}C sintered. Hardness of the composites was lower than that of pure HA powder based ceramics due to the presence of relatively high porosity. 10vol% MSS whisker addition yields comparable compressive strength (460-470 MPa) and elastic modulus values (14-17 GPa) with that of natural bone tissues (170-193 MPa compressive strength, 14-18 GPa elastic modulus).

ÖZ

Bu çalışmada hidroksiapatit (HA) tozlarının, viskerlerinin ve HA bazlı seramiklerin hazırlanması incelenmiştir. Ticari HA tozu karşılaştırma amacı ile kullanılmıştır. Tozlar ve sinterlenmiş seramikler optik mikroskop, SEM, XRD, tane buyot analizi, dilatometri ve mekanik testler kullanılarak karakterize edilmiştir.

Ca-P tozları sulu ortamda $(NH_4)_2HPO_4$ ve $Ca(NO_3)_2$. $4H_2O$ kullanılarak çökeltme yöntemiyle sentezlenmiştir. Ca/P oranı pH=10 da 60^oCde ve 24 saat yaşlandırma koşullarında 1,5 ve 1,67 ye ayarlanmış ve sırasıyla Ca-P fazları ve HA tozu elde edilmiştir. Ca/P oranı 1,67 ye sabitlenerek ortam pH sının, yaşlanma sıcaklığı ve zamanının toz özelliklerine olan etkisi incelenmiştir. Yaşlanma zamanı ve sıcaklığı sırasıyla 24 saat ve 60 ^oC de sabit tutularak pH 4,6,8,9,10 and 11 ayarlanmıştır. HA tozlarının oluşumu pH 8 den sonar gözlenmiştir. pH=4 aglomere olmuş Monetite-Brushite tozu elde edilmiştir. Prizmatik Brushite kristalleri pH=6 da elde edilmiştir. Yaşlanma zamanı incelemeleri 30-90 ºC de pH=10 a ve yaşlanma zamanı 24 saate sabitlenerek gerçekleştirilmiştir. Yaşlanma sıcaklığındaki artış ısıl olarak daha kararlı HA fazı olusumunu sağlamıstır. Çökeltiler pH=10 a ve sıcaklık 60 ºC ye sabitlenerek 0, 0.5, 1, 24 ve 48 saat boyunya yaşlandırılmıştır. Isıl olarak kararlı HA fazı 24 saat yaşlandırma sonrasında elde edilmiştir. Fırında kurutulan tüm çökeltiler ısıl kararlılıklarının ve faz yapısındaki gelişmelerin incelenmesi amacıyla 400-1250 ºC aralığında ısıl işleme tabi tutulmuşlardır. Isıl olarak kararlı HA tozlarının çökeltilmesi için pH=10, yaşlandırma sıcaklığı ve zamanı 60 ^oC, 24 saat optimum şartlar olarak belirlenmiş ve bu şartlarda eşboyutlu ve 40-60 nm tane boyutlarında HA tozları üretilmiştir

HA viskerleri hazırlamak için erimiş tuz sentezlemesi (MSS) ve hidrotermal sentezleme (HDT) yöntemleri kullanılmıştır. Her iki viskerinde XRD desenleri göstermiştir ki HA baskın fazdır ve baska fazlar bulunmamıştır. Hidrotermal viskerler mikronaltı captadırlar ve ortalama 20 aspect oranına sahiptirler. Çoğunlukla altıgen MSS viskerlerin çapları 1-5 mikron aralığındadır ve 10-15 aspect oranına sahiptirler.

10, 20 and 30 vol% visker içeren kompozitler hazırlanmıştır. Sinterlenme davranışları ve mekanik özellikleri incelenmiştir. 98% teorik yoğunluklu HA seramikleri (3.16 g/cm^3) 1150-1250^0C aralığında elde edilmiştir. MSS visker içeren kompozitler için 80-90% teorik yoğunluk 1200^0C üzerinde çok az bir küçülme ile

eldedilmiştir. HDT visker içeren kompozitlerin yoğunlukları MSS içerenlerinkinden daha fazlaydı. En yüksek sertlik değeri 1250^{o}C de sinterlenmiş HA seramiğinden 537 Hv olarak elde edildi. Göreceli yüksek gözeneklilik sebebiyle kompozitlerin sertlikleri saf HA seramiklerinden daha düşük olarak tespit edildi. 10vol% MSS visker eklenmesi doğal kemik dokusununkiyle (170-193 Mpa basma mukavemeti, 14-18 GPa elastik modulus) karşılaştırılabilecek basma mukavemeti (460-470 MPa) ve elastik modulus(14-17 GPa) değerlerini sağlamıştır.

TABLE OF CONTENTS

LIST OF TABLES

LIST OF FIGURES

CHAPTER I

INTRODUCTION

The emerging importance of ceramics in biomaterial applications in the past couple of decades has been stated by Dr.L.L.Hench as: “Many millennia ago, the discovery that fire would irreversibly transform clay into ceramic pottery led to an agrarian society and an enormous improvement in the quality and length of life. Another revolution has occurred in the use of ceramics during the past four decades to improve the quality of life. This revolution is the innovative use of specially designed ceramics for the repair, reconstruction and replacement of diseased or damaged parts of the body. Ceramics used for this purpose are termed bio-ceramics,” in his 1998 review article in the Journal of the American Ceramic Society on “Bioceramics” (1).

All humans start aging from the day they are born and are always likely to face traumatic or non-traumatic events, which may cause damage or loss of soft or hard tissues in their biological system. Biomaterials are either natural or synthetic materials used in a wide spectrum of medical and dental implant and prostheses applications for repair, augmentation or replacement of natural tissues. They should be biocompatible which necessitates the absence of local or body wide toxic, carciogenic, antigenic and mutagenic effects on the biological system (2). Biomaterials must also have sufficient durability under extreme physical and chemical conditions in the body (1-7).

Human body can be defined as a unique machine formed by the complicated cooperation of materials. One of the most important structural components of human body is the skeletal system that serves many important functions; it supports and protects our bodies, produces blood and stores minerals in addition to providing the shape and form for our bodies. A rigid framework to which soft tissues and the organs of the body are attached is formed by 206 bones of the skeletal system. Just like other well known conventional materials, bones also break, crack or wear out under extreme conditions. According to a statistical study conducted by the Turkish Ministry of Health (8) between the years 1987 to 1994, 85212 patients were hospitalized due to 40 different bone diseases. Although we do not know the exact number of the bone replacement and reconstruction operations and the related medical expenses in our country, it has been

reported that every year about half a million hip prostheses operations have been done and $2.3 billion have been spent for hard tissue replacement and reconstruction operations worldwide (2).

This growing need encouraged the materials engineers and researchers to conduct research and development towards a material that can be used as an implant material for the repair and replacement of hard tissues. Among all the materials offered by the recent technology, only the very small fraction can pass some biological and mechanical restrictions and be used as a biomaterial.

One of the most important materials to be used for hard tissue replacement operations is hydroxyapatite (HA) (1-7) which is the main mineral component of the human hard tissues. Synthetic HA powders with a composition of $Ca_{(10-x)}(HPO_4)_x(PO_4)_{(6-x)}(OH)_{(2-x)}$ $0 \leq x \leq 1$ is commonly prepared by various precipitation techniques. The powder properties may be directly affected by various precipitation parameters like Ca/P ratio of the starting reagents, pH, aging time and temperature, stirring conditions, addition rate of the reactants, etc (13, 14, 20, and 22). The preparation of HA ceramics with a fine microstructure and improved mechanical properties necessitates consolidation of unagglomerated nanosized particles with uniform particle size distributions

Despite its excellent bioactivity and biocompatibility, mechanical properties of HA are not sufficient enough to be used as load bearing replacement operations. The mismatch between the mechanical properties of the implant and the bone may cause stress concentration in the interface that may consequently end up with the death of the surrounding tissue especially in load-bearing implant applications. Human bone must be under a certain amount of load in order to remain healthy. When the bone is unloaded or overloaded in compression weakening of the bone and degradation of the bone-implant interface along with possible biological changes may occur (2, 9). Mechanical properties can be enhanced by the addition of different reinforcements like whiskers, fibers, particulates, etc.

The subject of this work was one of the initial stages of an ongoing DPT project at the Faculty of Engineering of IZTECH. The effect of pH, aging time and temperature on the HA powder properties were investigated in this work and the prepared powders were well characterized by using various techniques. The densification behavior and the

effect of HA whisker addition on the densification and the mechanical properties of the HA ceramics were investigated in the second part of this work.

CHAPTER II

STRUCTURE AND PROPERTIES OF HARD TISSUES

Skeletal system is one of the most important components of our body and is formed of 206 bones. The hard tissues i.e., bones and teeth (Figures 1, 2, 3), are composed of inorganic and organic phases with complex microstructures (2). Although it is rather difficult to determine the bone composition due to presence of many levels of organizations, it consists mainly of 20 w/w % collagen, 69 w/w % calcium phosphate, 9 w/w % water and other organic materials. Collagen in the form of small microfibers forms the matrix constituent of the bone. The diameter of the collagen microfibers varies from 100-2000 nm. Calcium phosphate in the form of hydroxyapatite crystals, which are about 40-60 nm in length, 20 nm in width and 1.5-5 nm in thickness, provides stiffness to the bone. HA crystals are arranged parallel to the long axis of collagen fibers. Bone consists of two main parts, compact bone and cancellous bone (Figure 1). Compact bone is harder and denser compared to cancellous bone with different microstructures (Figure 2). Cancellous bone is active metabolically and is remodeled more often than compact bone. Because of the directional arrangement of collagen fibers and HA crystals, bone displays anisotropic mechanical properties (Table 1)(2).

Tooth consists of two parts, which are the crown and the root (Figure 3). The root is covered by a layer of cementum attached to the bone by periodontal membrane (a layer of fibrous connective tissue). Enamel and dentine form the main two parts of the crown. The enamel is the hardest substance in the body and consists of 97w/w % relatively large HA crystals (25nm thick, 40-120 nm wide, and 160-1000nm long) and the remaining part organic substances and water. Dentine is the mineralized tissue similar in composition to regular compact bone (2).

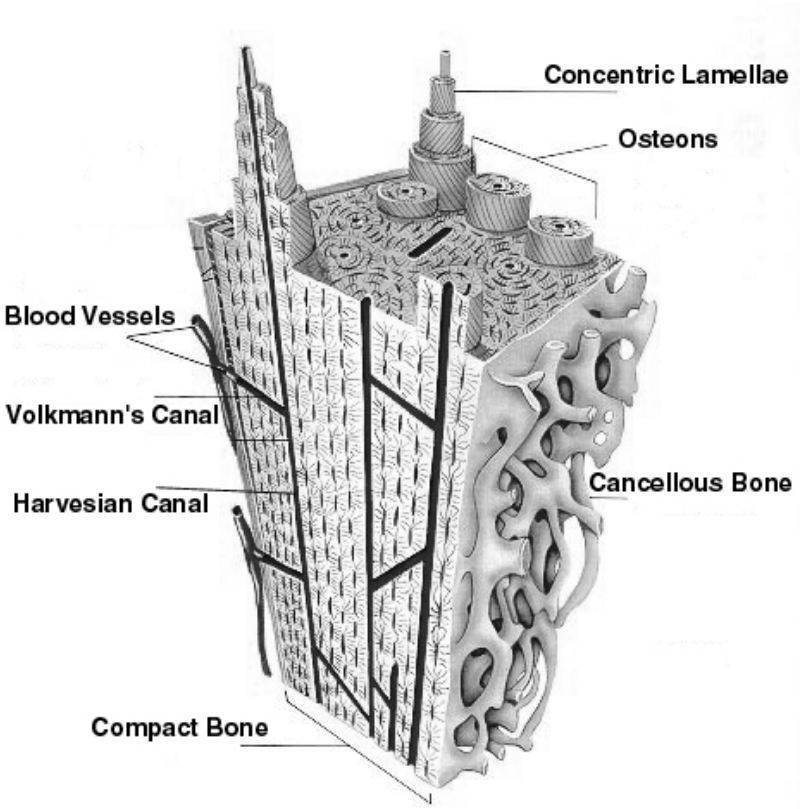

Figure 1. Schematic presentation of compact bone cross-section.

Bones have to carry our weight for lifetime and our teeth must work under stress of about 20 MPa applied 3000 times a day without fatigue and only with moderate wear (2). Mechanical properties of bone and teeth are summarized in Tables 1 and 2 respectively. Chemical composition of the hard tissues is also very important in determining their properties and functions. The main elements present in the bone are Ca , P and O, and there are also considerable amounts of Na^+, Mg^{2+}, K^+, CO_3^{2-}, F^-, Cl^- and H_2O. The chemical compositions of the hard tissues are summarized in Table 3 (2).

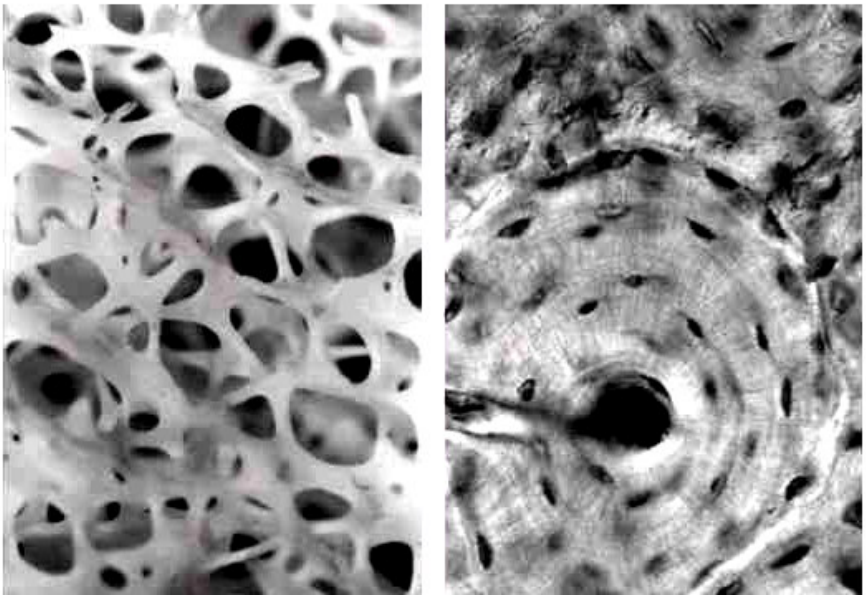

Figure 2. Micrograph of the cancellous and compact bone structure.

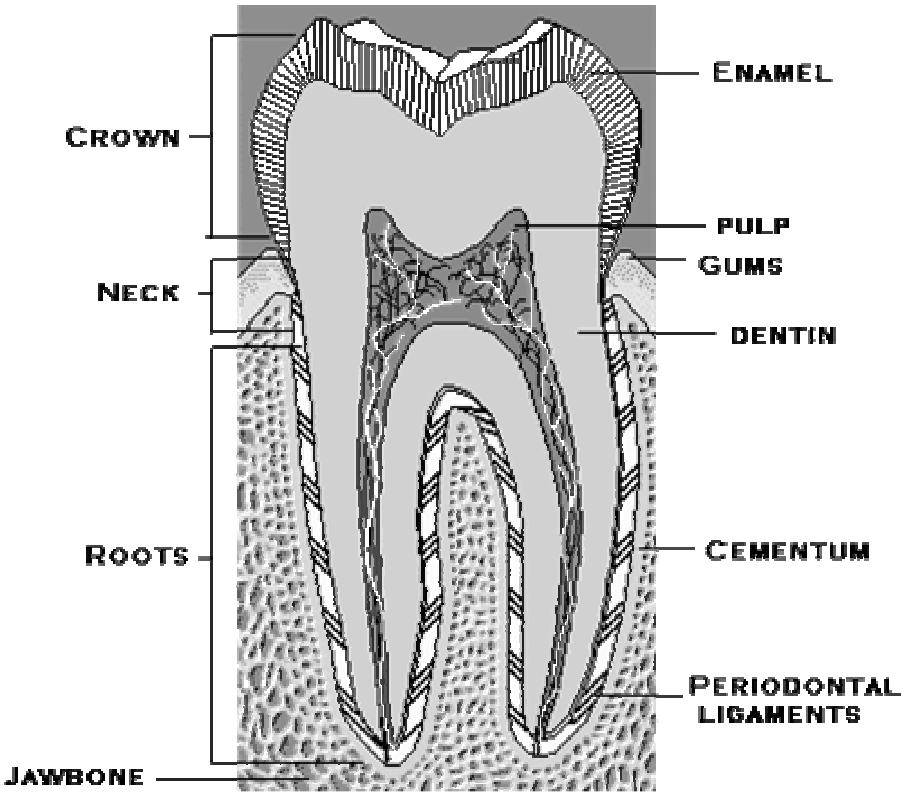

Figure 3. Schematic presentation of human tooth cross-section.

Table 1. Mechanical properties of a compact human bone (2).

	Test direction related to	bone axis
	Parallel	normal
Tensile strength (MPa)	124-174	49
Compressive strength (MPa)	170-193	133
Bending strength (MPa)	160	
Shear strength (MPa)	54	
Young's modulus (GPa)	17.0-18.9	11.5
	20-27(random)	
Work of fracture (J/m^2)	6000 (low strain rate)	
	98 (high strain rate)	
K_{IC} ($MPa.m^{1/2}$)	2-12	
Ultimate tensile strain	0.014-0.031	0.007
Ultimate compressive strain	0.0185-0.026	0.028
Yield tensile strain	0.007	0.004
Yield compressive strain	0.010	0.011

Table 2. Mechanical properties of human tooth (2).

	Dentine	Enamel
Compressive strength (Mpa)	250-350	95-370
Proportional limit in compression (MPa)	160-170	70-350
Young's modulus in compression (GPa)	11-17	9-84
Tensile strength (MPa)	21-53	10
Young's modulus in tension (GPa)	11-19	.....
Flexural strength (Mpa)	245-268	76
Young's modulus in bending (GPa)	12	131
Shear strength (MPa)	69-147	64-93
Proportional limit in shear (MPa)	60	.....
Shear modulus (GPa)	6	.....
Work of fracture (J/m^2)	200-500	13
		200

Table 3. Chemical composition and crystallographic parameters of human bone and tooth (2).

	Enamel	Dentine	Bone
Composition W %			
Calcium Ca^{2+}	36.5	35.1	34.8
Phosphorus as P	17.7	16.9	15.2
Ca/P molar	1.63	1.61	1.71
Sodium Na^{+}	0.5	0.6	0.9
Magnesium Mg^{2+}	0.44	1.23	0.72
Potassium K^{+}	0.08	0.05	0.03
Carbonate as CO_3^{2-}	3.5	5.6	7.4
Fluoride F^{-}	0.01	0.06	0.03
Chloride Cl^{-}	0.30	0.01	0.13
Pyrophosphate $P_2O_7^{4-}$	0.022	0.10	0.07
Total inorganic (mineral)	97.0	70.0	65.0
Total organic	1.5	20.0	25.0
Absorbed H_2O	1.5	10.0	10.0
Trace elements Sr^{2+},Pb^{2+},Zn^{2+} Cu^{2+},Fe^{3+}			
Crystallographic properties			
Lattice parameters (±0.003 Angs)			
a-axis	9.441	9.42	9.41
c-axis	6.880	6.88	6.89
Crystallinity index	70-75	33-77	33-37
Crystallite size (aver), Angs	1,300x300	200x40	250x30
Ignition products (800 ^{o}C)	β-TCP+ HAp	β-TCP+ HAp	HAp+CaO

CHAPTER III

BIOMATERIALS

Biomaterials are either natural or synthetic materials used in a wide spectrum of medical and dental implant and prosthesis applications for repair, augmentation or replacement of natural tissues (5). Biomedical devices or implants can be classified according to their biologic responses; bio-inert, bioactive and bio-resorbable. Bio-inert materials do not show any negative reactions but encapsulated by the surrounding tissue (morphological fixation). However bioactive materials display a perfect interfacial bonding to the tissues or allow ingrowth of tissue into a material (bioactive fixation). Bioresorbable materials replaced by the tissues in / on which they are implanted (replacement).

Biomaterials can be classified as conventional materails: polymers, metals, ceramics and composites which are now being specifically developed for medical applications

3.1. Bioceramics

Advanced ceramics are finding unique applications in biomedical industry besides their potential and current uses in various other high technology related fields. Ceramics engineered for biomedical applications are called bioceramics (1). Bioceramics are produced in a variety of forms and phases and serve many different functions in repair of the body, which are summarized in Figure 4 and Table 4. Ceramics, which are used in a bulk form of a specific shape, are called implants, prostheses or prosthetic devices. Bioceramics are also used to fill space while the natural repair process restores function. In some cases ceramics can be used as coating on other substrate or as a second phase in composite materials.

Depending on the properties or functions required, bioceramics could be fabricated in many different phases. Bioceramics can be single crystals (sapphire), polycrystalline (alumina, zirconia or hydroxyapatite), glass (Bioglass®), glass-ceramics (A/W glass ceramics) or composites (polyethylene- hydroxyapatite) (9).

The first reported clinical application of ceramics was the use of alumina as hip prostheses with an alumina head and socket in 1971 (9). Many different ceramics have been developed for very different types of clinical applications since the pioneering hip prostheses. The discovery of bioactive bonding mechanism to bone by L.L.Hench in 1969 and the discovery of bioactive bonding mechanism to soft tissue in the early 1980's (1-3) can be stated as the most important milestones in the bioceramic applications history. The first clinical applications of bioactive bonding have been done with the Bioglass® MEP in 1985 (9).

The term bioactive is specific only to ceramics since none of the other materials can display such a characteristic. As mentioned in the previous chapters biological response to the implant is one of the most important factors. No material implanted in living tissue is completely inert and all materials elicit a response from host tissues. Depending on the type of tissue response bioceramics can be classified as in Table 4 (3).

Today lots of ceramics have been used for the repair and reconstruction of the diseased part of human skeletal system. Ceramics like alumina, zirconia, HA or HA coated metals have been used for the restoration operations of the load carrying parts of the skeletal system (Figure 4). Particularly, for the load bearing implantation operations, besides the biological response, mechanical matching with the bone is one of the most important factors for the survivability of the implant. Existence of the mechanical mismatch may cause a stress concentration in the bone – implant interface where consequently death of the surrounding tissue may be observed. The design of a material with similar mechanical properties with the replaced bone tissue is very important for the quality of the lives of the patients.

Table 4. Types of bioceramics related to their biological responses (3).

Type of bioceramics	Type of attachment	Example
1	Dense, nonporous nearly inert ceramics attach by the bone growth into surface irregularities, by cementing the device into the tissues, or by press fitting into e defect (termed morphological fixation)	Al_2O_3 (singe crystal and polycrystal)
2	For porous inert implants, bone ingrowth occurs, which mechanically attaches the bone to the material (termed biological fixation)	Al_2O_3 (porous polycrystalline) hydroxyapatite coated porous metals
3	Dense, nonporous surface reactive ceramics, glasses and glass-ceramics attach directly by chemical bonding with the bone (termed bioactive fixation)	Bioactive glasses, bioactive glass-ceramics, hydroxyapatite
4	Dense, nonporous or porous resorbable ceramics are designed to be slowly replaced by bone	Calcium sulfate(plaster of Paris), tricalcium phosphate, calcium phosphate salts

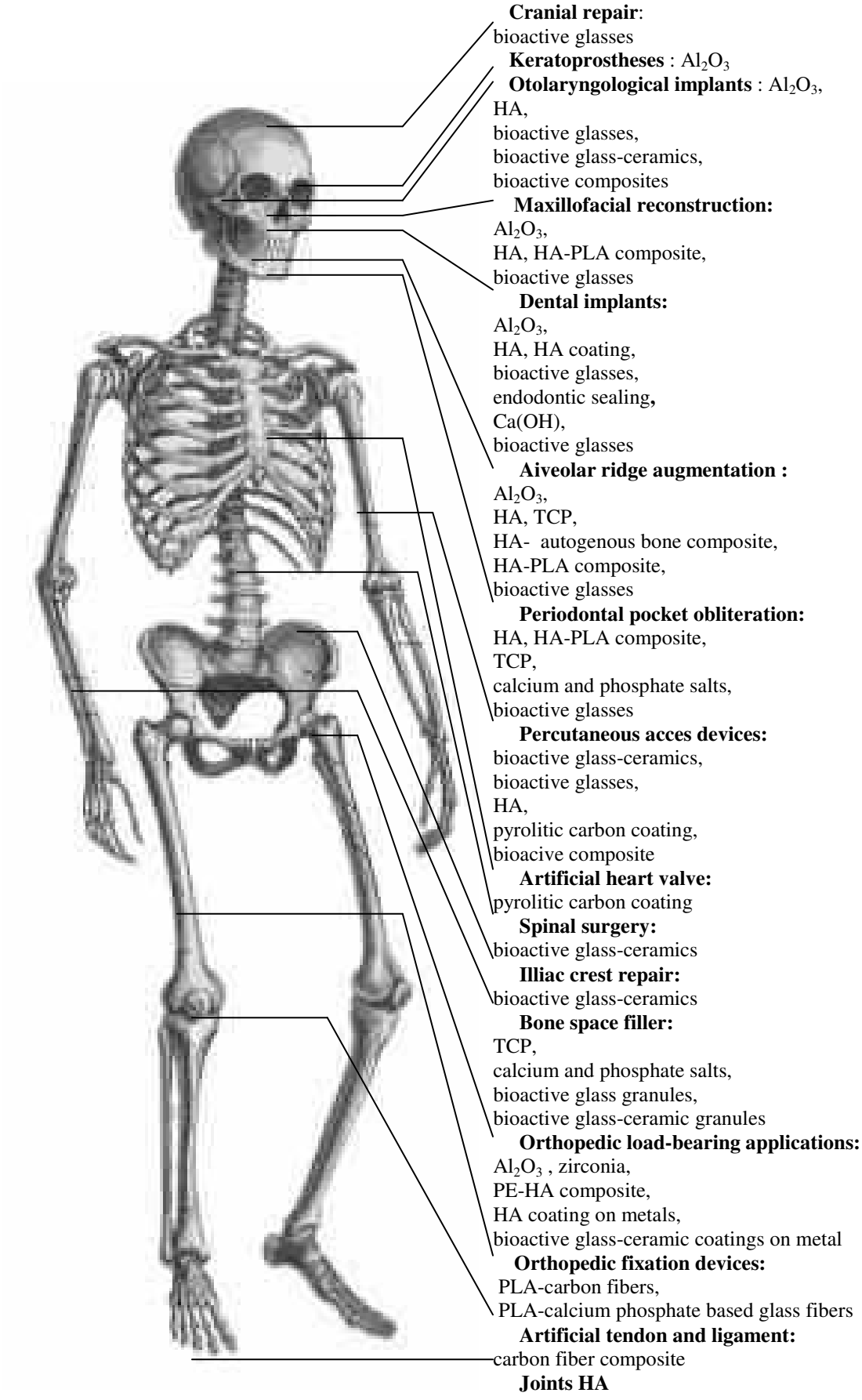

Figure 4. General usage of bioceramics (11)

3.2.1. Alumina and Zirconia as a Ceramic Biomaterial

Both alumina and zirconia are exceptional candidates for biomedical load-bearing applications with their own superb mechanical properties and biocompatibility due to chemical inertness in the body environment. These two ceramics are especially used for fabrication of hip ball for the total hip replacement operations. In load-bearing operations the major limitation comes from the mechanical mismatch with the bone and implant material. In order to remain healthy, bone must be under a certain amount of load, but high modules of elasticity of both ceramics shield the bone from mechanical loading since most of the loads carried by the implant. If the bone is unloaded or loaded in compression may cause biological changes, which leads to resorbtion or weakening of the bone and degradation of bone-implant interface. Elastic modulus of both ceramics is a limitation on their use in the body. The young's modulus of cancellous bone has a range from 0.05 to 0.5 GPa and cortical bone ranges from 7 to 25 GPa depending on location and age (11, 2, 9). In contrast, young's modulus for alumina and zirconia ranges from 380 to 420 and from 150 to 208 GPa respectively (10). Mechanical properties of alumina and zirconia are listed in Table 5. Moreover, the phenomena of slow crack growth, static and cyclic fracture, low toughness, stress corrosion, deterioration of toughness with time and sensitivity to tensile stresses are all serious concerns for both ceramics. Thus they are restricted to designs involving compressive loading or limited tensile loads.

Despite the above restrictions, alumina and zirconia are exceptional materials for the total hip replacement operations. More than one-half million alumina and 300.000 TZP ball heads have been implanted and only 5 and 2 failures reported respectively up to now. The minimal requirements for alumina and zirconia as an implant material are described by ISO 6474, ISO 13356 (9, 10,11) respectively (Table 5).

Table 5. Characteristics of some ceramics for biomedical applications(10).

Property	Alumina	Mg-PSZ	TZP
Chemical composition	99,9% Al_2O_3 +MgO	ZrO_2 +8-10 mol % MgO	ZrO_2 +3 molY_2O_3
Density g/cm^3	>3,97	5,74-6	>6
Porosity %	<0,1	-	<0,1
Bending strength MPa	>500	450-700	900-1200
Compression strength MPa	4100	2000	2000
Young modulus GPa	380	200	210
Fracture toughness K_{IC} MPa.m$^{1/2}$	4	7-15	7-10
Thermal expansion coeff.. K^{-1}	8x10^{-6}	7-10x10^{-6}	11x10^{-6}
Thermal conductivity WmK^{-1}	30	2	2
Hardness HV 0,1	2200	1200	1200

CHAPTER IV

HYDROXYAPATITE (HA)

An average 70 kg man has about 780 g P in his body 700 g of which is present as bone apatite. This means that an average man has 3.5-4 kg hydroxyapatite in his body (12). Among all available materials hydroxyapatite, which is the main inorganic component of hard tissues, seems to be the most suitable material for hard tissue replacement operations because of its excellent biocompatibility and bioactivity.

4.1. General Properties and Structure of Calcium Hydroxyapatite

The term *Apatite* describes a family of compounds with similar structures but not necessarily with identical compositions. Hence, apatite is a description not a composition. Hydroxyapatite (hydroxylapatite), $Ca_{10}(PO_4)_6(OH)_2$ (sometimes used as $3Ca_3(PO_4)_2 .Ca(OH)_2$), is the most important member of compounds which can be represented by the formula $M_{10}(XO_4)Y_2$, where M can be various metals or H_3O^+ , X= P, As, Si, Ge, S, Cr and Y=OH, F, CL, Br, CO_3 etc. (12).

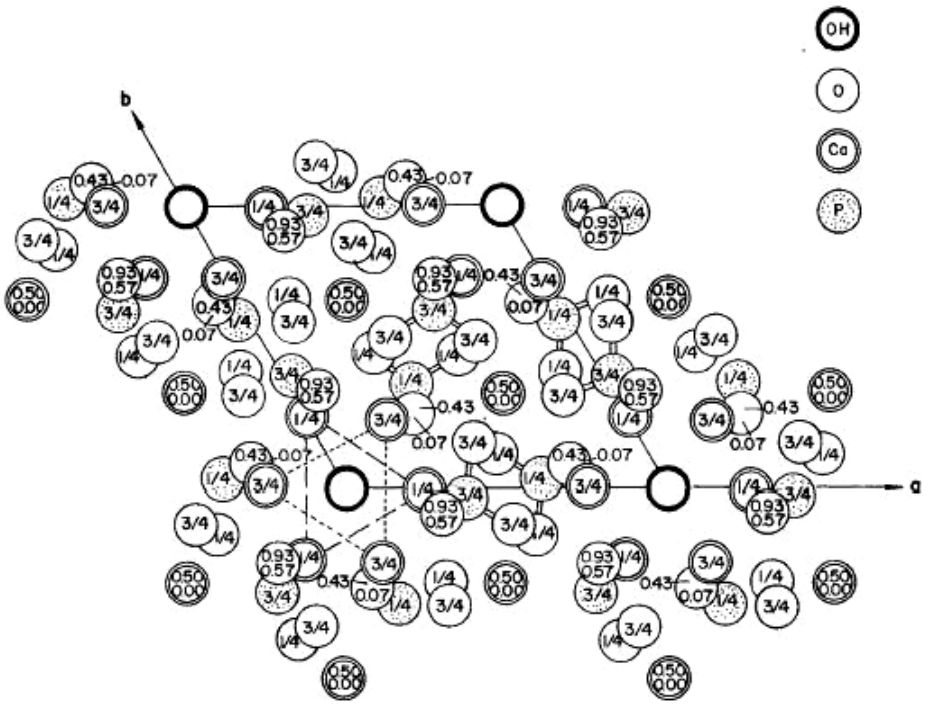

Figure 5. Unit cell drawing of HA crystal c-axis projection (12).

Apatite compounds have the same type of hexagonal structures with a space group $P6_3/m$. This space group is characterized by a six-fold c-axis perpendicular to three equivalent a-axis (a_1, a_2, a_3) at 120º to each other. The smallest building unit, known as the unit cell, contains a complete representation of HA crystal. The structure consists of Ca, PO_4, and OH groups closely packed together. Ten calcium atoms belong to either Ca(I) or Ca(II) subsets depending on their environment. Four calcium atoms occupy the Ca(I) position: two at level z=0 and two at z=0.5. Remaining six atoms occupy the Ca(II) positions: one group of three calcium atoms describing a triangle located at z=0.25, the other group of three at z=0.75, surrounding the OH groups located at the corners of unit cell at z=0.25 respectively. The six phosphate (PO_4) tetrahedra are in helical arrangement from levels z=0.25 to z=0.75. Powder HA gives an XRD pattern (Figure 6) characterized by diffraction peaks with small line broadening ($B_{1/2}$) and high intensities indicating a high degree of crystallinity. The lattice parameters are a=9.422 and c=6.881 ± 0.003 Å.

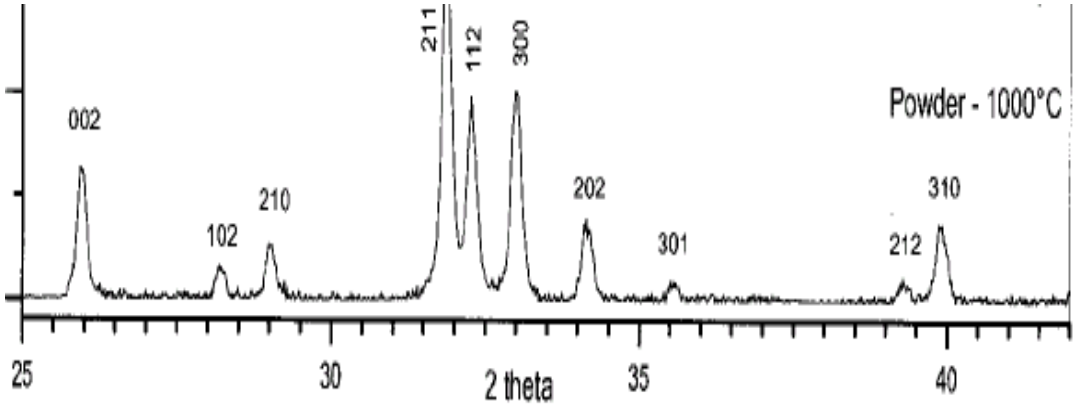

Figure 6. XRD pattern of stoichiometric HA powder.

4.2. Preparation of Hydroxyapatite Powders

Pure HA can be obtained from reactions in aqueous media or from solid-state reactions. Solid-state reactions yield stoichiometric and well-crystallized powders but they require relatively higher temperatures and longer heat treatment times and sinterability of these powders is very low (2).

Pure HA has a theoretical composition of 39.68w/w % Ca and 18.45w/w % P with a Ca/P molar ratio of 1.667 (Ca/P weight ratio of 2.151)(9). The only phase stable in the physiological environment existing in the $CaO\text{-}P_2O_5\text{-}H_2O$ ternary system is HA. A list of phases in the $CaO\text{-}P_2O_5\text{-}H_2O$ ternary system is given in Table 6 (12). Stability of HA based materials in the body environment and at elevated temperatures significantly depends on the stoichiometry of the HA. HA precipitated from aqueous solutions is generally expressed as $Ca_{(10-x)}\ (HPO_4)_x\ (PO_4)_{(6-x)}\ (OH)_{(2-x)}\quad 0 \leq x \leq 1$. Temperature, pH and the concentrations of the reactants, ageing time and temperature are the major factors effective on the stoichiometry, crystallinity and the morphology of the powders. Wet methods like precipitation (2, 13-22), hydrothermal technique (23-28), hydrolysis of other calcium phosphates (29-31) or other various techniques like sol-gel (43,44), flux method (32), electro-crystallization (33), spray-pyrolysis, freeze-drying, microwave irradiation, mechano-chemical or emulsion processing (42) can be used for HA powder preparation.. A typical SEM micrograph of a precipitated stoichiometric HA powder is given in Figure 7.

Figure 7. SEM micrograph of the as synthesized HA powder (Ca/P=1,667) (13)

Table 6. Phases present in the $CaO-P_2O_5-H_2O$ ternary system (12).

Chemical formula	Ca/P ratio	Name
$Ca(H_2PO_4)_2$	0.5	Monocalcium phosphate
$Ca(H_2PO_4)_2.H_2O$	0.5	Monocalcium phosphate monohydrate
$CaHPO_4$	1.0	Monetite (dicalcium phosphate)
$CaHPO_4.1/2\ H_2O$	1.0	Dicalcium phosphate hemihydrate
$CaHPO_4.2\ H_2O$	1.0	Brushite
α-$Ca_3(PO_4)_2$	1.5	α-tricalcium phosphate
β- $Ca_3(PO_4)_2$	1.5	Whitlockite
$Ca_{10}(PO_4)_6(OH)_2$	1.67	Hydroxyapatite
$Ca_2PO_4(OH)2H_2O$	2.00	Hydroxyspodiosite
$Ca_8H_2(PO_4)_6.5H_2O$	1.33	Octacalcium phosphate
$Ca_3(PO_4)_2.CaO$	2.00	Tetracalcium phosphate

The HA precipitation methods commonly used in commercial preparations are basically based on two methods outlined by Rathje, Hayek and Newesely (9). The first method involves the dropwise addition of phosphoric acid (H_3PO_4) to an aqueous suspension of calcium hydroxide ($Ca(OH)_2$) under constant stirring. The overall precipitation reaction can be expressed as follows:

$$10Ca(OH)_2 + 6\ H_3PO_4 \longrightarrow Ca_{10}(PO_4)_6(OH)_2 + 18\ H_2O$$

The above precipitation reaction medium is further controlled by the addition of NH_4OH to keep the pH of the solution alkaline to insure the formation of HA. The second method involves the reaction between calcium nitrate and ammonium phosphate in ammonium hydroxide added aqueous medium as follows (18, 19):

$$10Ca(NO_3)_2.4H_2O + 6(NH_4)_2HPO_4 + 8NH_4OH \longrightarrow$$

$$Ca_{10}(PO_4)_6(OH)_2 + 20NH_4NO_3 + 6H_2O$$

The precipitated powder properties, the nature and crystallinity of the phases present in the resultant powders prepared by the second method depends significantly on the temperature, pH, time and other precipitation conditions (13, 22, 19, 14). The pH of the starting solutions can affect the kinetics of precipitation and primary particle agglomeration because of the changes in the saturation levels of the HA. As the pH increases, a preferred growth along <002> axis of HA is observed which results in rod like morphology and relatively larger average particle sizes (22). Similarly as the pH increases from acidic to alkaline values, the Ca/P ratio of the powder becomes closer to the stoichiometric 1.667 values. The precipitate produced at pH=10.4 resulted in well stoichiometric HA that was sintered to 98.5% of theoretical density whereas at lower and higher pH values non-stoichiometric HA powders and phase decomposition during sintering was observed (22).

It was reported that the aging is critical towards obtaining well crystallized HA particles with uniform morphologies (20, 24). Impurities are removed, crystal strain is reduced, grains with non-uniform morphologies redissolve and they are re-crystallised into more ordered forms during aging. Longer aging times also ensure that the reagents are fully reacted and precipitated. Ahn and et al.(22) noted that an aging period of 100 hours led to a small crystallite size (~50nm) and high surface area (~90 m^2/g) for the calcined powder at 550 ºC . This aged powder was further sintered without phase decompositions whereas unaged precipitate phase was not thermally stable due to its poor compositional uniformity.

The variation of Ca/P ratio with time at 35 ºC is given in Figure 8. The phase transformations occurring during precipitation were discussed in detail by Lui et al. (20). At the initial stage of the precipitation reaction an unstable phase called as octacalcium phosphate (OCP $Ca_8H_2(PO_4)_6.5H_2O$) forms and rapidly transforms into amorphous calcium phosphate (ACP $Ca_3(PO_4)_2.x\ H_2O$ Ca/P=1.5). In the second stage of the precipitation reaction ACP transforms into calcium-deficient hydroxyapatite (DAP $Ca_{10-x}(HPO_4)_x(PO_4)_{6-x}(OH)_{2-x}.\ nH_2O$ $0 \leq x \leq 1$). DCP gradually becomes stable HA ($Ca_{10}(PO_4)_6(OH)_2$ Ca/P=1.67) during the aging process. The sequence of phase transformations can be summarized as: OCP→ACP→DAP→HA.

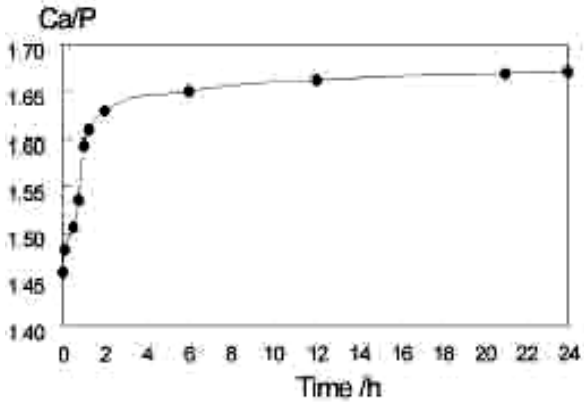

Figure 8. The variation of Ca/P ratio with time at 35 ºC (20).

The precipitation temperature also affects the rate of the reaction/transformations and the morphology of the precipitate. The formation ratio of HA during the precipitation with respect to time and temperature was given as shown in Figure 9. Increase in the temperature accelerates the formation of HA and decreases the time required to produce phase pure HA as shown in Figure 10. Formation of HA at 25ºC was reported to be about 24 hours while it took about 5 minutes at 60 ºC. The particle size of HA was determined ~10nm at 15ºC while it was about 100 nm at 60 ºC (20) and SEM micrographs of these powders is given in Figure 11.

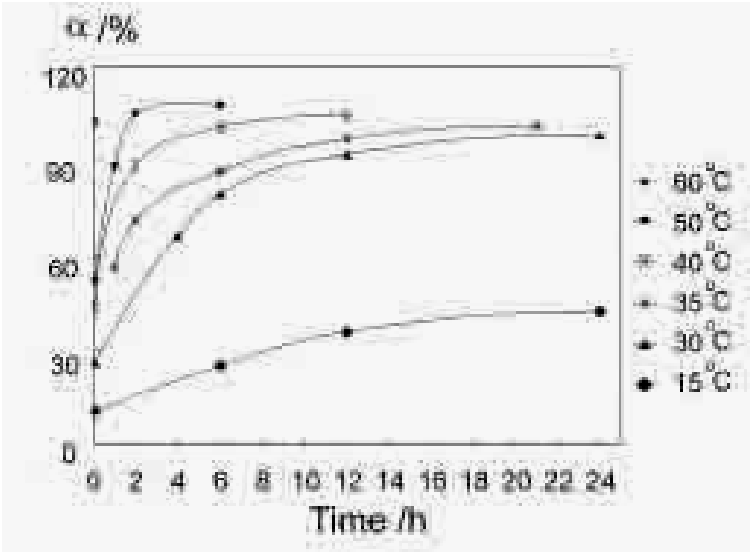

Figure 9. Relationship between the formation ratio of HA and reaction time under different temperatures (20).

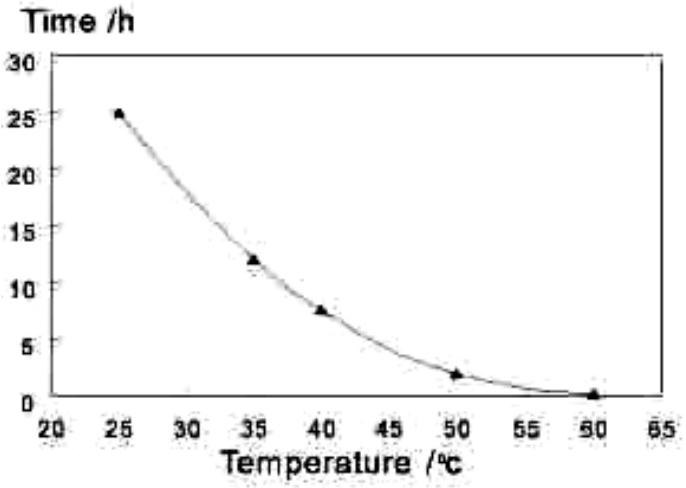

Figure 10. Relationship between the time required for forming pure-phase HA and temperature (20)

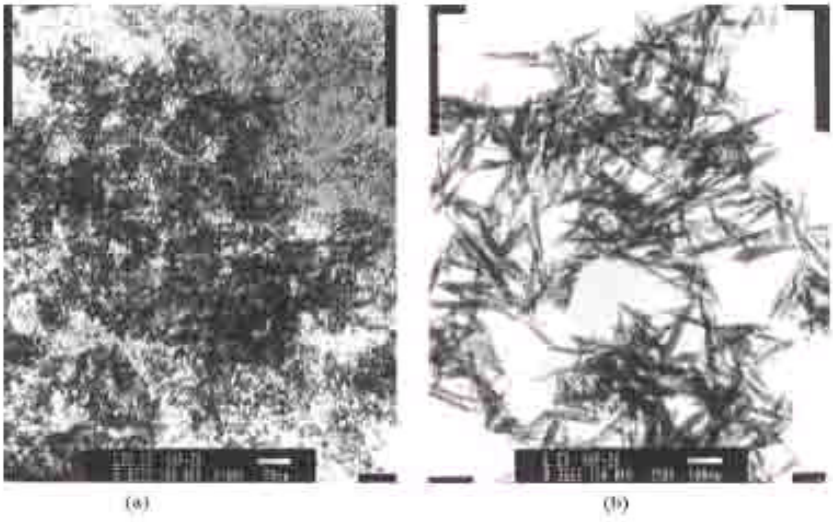

Figure 11. Influence of reaction temperature on the morphology of HA a) 15 ºC b) 60 ºC (20)

HA can also be prepared by the hydrolysis of $CaHPO_4$, $CaHPO_4.1/2\ H_2O$, $CaHPO_4.2H_2O$, β and α-$Ca_3(PO_4)_2$, $Ca_2PO_4(OH)2H_2O$, $Ca_8H_2(PO_4)_6.5H_2O$, $Ca_3(PO_4)_2.CaO$, generally to form a calcium deficient HA. A solid state reaction of some calcium phosphate compounds with the $Ca(OH)_2$ yield stoichiometric HA above 950^0C (2,34,35,36).

4.2.1. Preparation of HA Whiskers

Inorganic fibers and whiskers have been used for many years in a variety of applications mostly as reinforcements in composites. Various fibrous materials, such as carbon, glass, SiC, Si_3N_4, Al_2O_3, ZrO_2 and many others have been prepared for this purpose. According to Stanton and Pott criteria fibrous materials are restricted in dimensions to diameters <1μm and length >10 μm for possible use in the human body with no carcinogenic effects (2). Most of the commercially available whiskers cannot fulfill this criterion and the main limitation is their chemical composition and their biological inertness. Currently HA whiskers may be the most suitable materials as reinforcements in composites since they may fulfill the above conditions. HA whiskers contain only non-toxic species and although they have a dangerous geometry, they dissolve in human body without causing any health problems.

Preparation techniques for HA whiskers can be divided into three groups: the homogeneous precipitation using urea (2), the decomposition of chelating agents (25-27) and the molten salt synthesis (32). The first method utilizes a continuous increase of pH in the solution containing calcium and phosphate ions at high temperatures.

The principle of the decomposition of chelating agents is based on the controlled release of Ca^{2+} ions into a medium generally under hydrothermal conditions. EDTA, lactic acid or citric acid are the commonly used materials as chelating agents. This method allows the formation of whiskers with a wide range diameter in the 0.1-5 μm and length in the 10-100 μm range. Ca/P ratio of such whiskers varies in the range of 1.59-1.63 deviating from the stoichiometric value of 1.67. The nature of the phases and the morphology of the prepared whiskers depend on the pH, temperature, concentration of reactants and the synthesis time. The precipitation reaction of HA whiskers in this method are based on the thermal dissociation of Ca-EDTA chelate as follows:

$$Ca(EDTA)^{2+} \rightarrow Ca^{2+} + EDTA^{4+}$$

$$5Ca^{2+} + 3PO_4^{3-} + OH^- \rightarrow Ca_5(PO_4)_3OH$$

Table 7. Relationship among pH, crystalline phase and critical precipitation temperature (27).

pH	Crystalline phase	Critical precipitation tempereture ºC
2	$CaHPO_4$	210
4	$CaHPO_4$	160
6	$Ca_5(PO_4)_3OH$	170
8	$Ca_5(PO_4)_3OH$	180
10	$Ca_5(PO_4)_3OH$	130

EDTA is stable up to about 200 ºC but as the temperature increases it starts to decompose slowly. HA phase can be precipitated if the pH and the temperature of the system is at certain levels. The relationships between pH, temperature and precipitated phase under hydrothermal conditions for such a system are summarized in Table 7. A typical SEM micrograph of the whiskers prepared by this method is given in Figure 12.

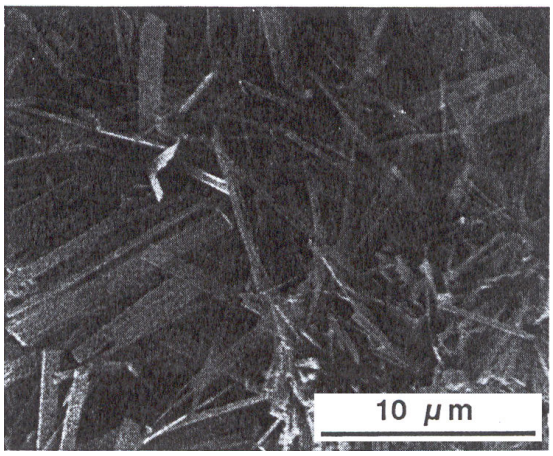

Figure 12. SEM micrograph of the HA obtained from Ca-EDTA and $(NH_4)_2HPO_4$ under hydrothermal conditions at 200^0C (26)

Molten salt synthesis (MSS) presents another approach for the preparation of HA whiskers. The MSS technique is based on the use of low temperature melting solvents such as alkali chlorides, sulfates, carbonates or hydroxides, as the medium of

whisker synthesis. This process can be summarized as the dissolution and re-crystallization of HA in the molten flux medium at or above its melting temperature. This process can be outlined in the following steps (32):

1. The liquid phase formed during the MSS process by the flux dissolves all of the HA powder first in the initial stage.
2. With further heating particles of the apatite phase are formed through the nucleation and growth processes.
3. As the molten ionic bath cools, while passing through its melting point down to room temperature, rapid crystallisation occurs along the preferred growth axis of the ceramic phase.

Figure 13. SEM micrograph of HA whiskers prepared by MSS (32).

Soaking time and temperature, superheating and the solubility of the HA in the molten flux all must have important effects on the crystallization process and the properties of the synthesized whiskers (32). The growth of HA whiskers during the MSS process is likely to occur by a dissolution-nucleation-crystal growth process where dissolution is likely to occur during the growth of the whiskers in the molten salt. The whiskers prepared by the MSS process had a high degree of crystallinity and relatively large aspect ratios. A typical SEM micrograph of MSS HA whiskers is given in Figure 13 and XRD patterns of starting powder and MSS whiskers are given in Figure 14.

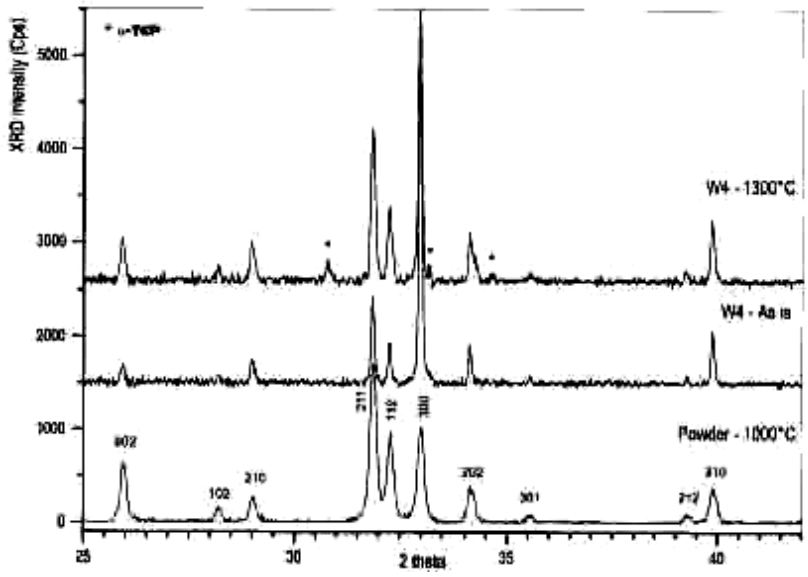

Figure 14. XRD patterns of calcined HA powders and HA MSS whiskers (32).

4.3. Consolidation and Sintering of Hydroxyapatite

The hydroxyapatite powders prepared by one of the methods summarized above can finally be processed into relatively dense or macroporous ceramics. Dense hydroxyapatite is generally defined as a ceramic with less than porosity of 5 vol.% (9). Hydroxyapatite powder can be compacted by uniaxial dry pressing in a die. Small amounts of low molecular weight hydrocarbons (3-5w/w %) can be used as a binder with 3-6w/w % water. Depending on the powder characteristics, HA powders can be compacted to 40-60% of theoretically dense green bodies under 80-160 MPa compaction pressures. Alternative ceramic powder consolidation techniques, such as cold isostatic pressing, extrusion, slipcasting (40,41), tape casting (36), can be used for the preparation of ceramics with more complex geometries.

Macroporous HA ceramics can be prepared by consolidating the HA powders with organic additives that will decompose during heating the compacts which may create controlled size pores in the compact proportional to the initial organic phase particle size. Hydrogen peroxide, naphthalene or some polymers like PE can be used as pore creating additives. These additives decompose and are removed from the compacts at heat treatment temperatures which are significantly lower than the HA sintering temperatures. Controlled porosity ceramic structures may be prepared as a result of

these processes (2,9). HA whiskers can also be compacted to produce similar highly porous HA ceramics.

Most of the HA powders can be densified to about theoretical density (3.16 g/cm^3) with pressureless sintering. Sintering temperatures vary between 900-1300 ºC with varying heating regimes depending on the powder characteristics and consolidation method utilized. The variation of the sintered density with temperature for uniaxially pressed HA powders is given in Figure 15. The dependence of the compressive strength on sintering temperature and density is also shown in the same graph. Exaggerated grain growth and the decomposition of the HA into TCP phase are the main issues to be considered in the selection of the sintering temperature and schedules (38). Alternatively hot pressing (HP) or hot isostatic pressing (HIP) techniques can also be used for the sintering of HA powder compacts.

4.4. Mechanical Properties of Hydroxyapatite

Dense phase pure HA ceramics are the most suitable implant materials because of their excellent biocompatibility. Mechanical properties and especially the fracture toughness and tensile strength of these ceramics are not unfortunately sufficient enough to be used as load bearing implant materials. Weibull modulus (m), which describes the reliability of ceramics, of HA ceramics is reported to be between 5-18 indicating that they behave as a typical brittle ceramic and the slow crack growth coefficient describing the resistance to fatigue failure is reported as 26-80 in dry conditions and 12-49 under wet conditions (2). This drop indicates the high susceptibility for slow crack growth under wet conditions. This property makes HA ceramics an unsuitable material for load bearing applications and the use of HA is mainly limited to powders, coatings, porous bodies and non-load bearing implants.

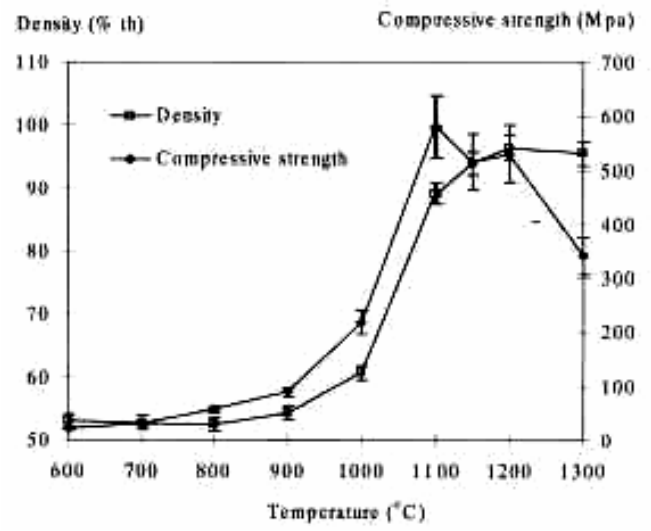

Figure 15. Relationship between the density and compressive strength of HA ceramics sintered at different temperatures (19).

The properties of the HA powder, consolidation and sintering conditions influence the mechanical properties of hydroxyapatite ceramics. Due to its complex composition and crystal structure HA ceramics are very sensitive to nonstoichiometry and impurities. Nonstoichiometry may cause the decomposition of HA into TCP phase at elevated temperatures. Formation of the new phase and the removal of water influence the densification behaviour of HA ceramics which may consequently cause the mechanical properties (39,51,15).

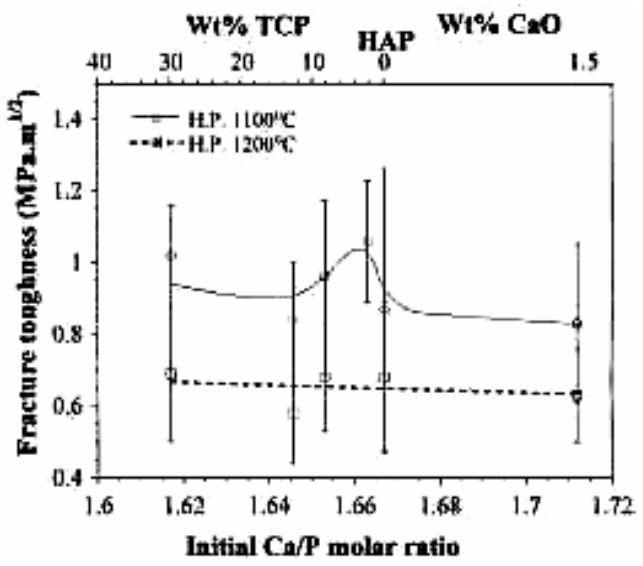

Figure 16. Relationship between the initial Ca/P ratio and fracture toughness of the HA ceramics HP at 1100 and 1200 ºC (37).

Fracture toughness of the dense phase pure HA is in the 0,8-1,2 range with an average of 1MPa $m^{1/2}$. It decreases dramatically with increasing porosity. Fracture energy is in the range of 2,3-20 J/m^2(2,52). The variation of the fracture toughness with Ca/P ratio for hot pressed HA ceramics sintered at two different temperatures are given in Figure 16 (37). The mechanical properties of HA ceramics are further compared with various other biomaterials and human bone in Figure 17.

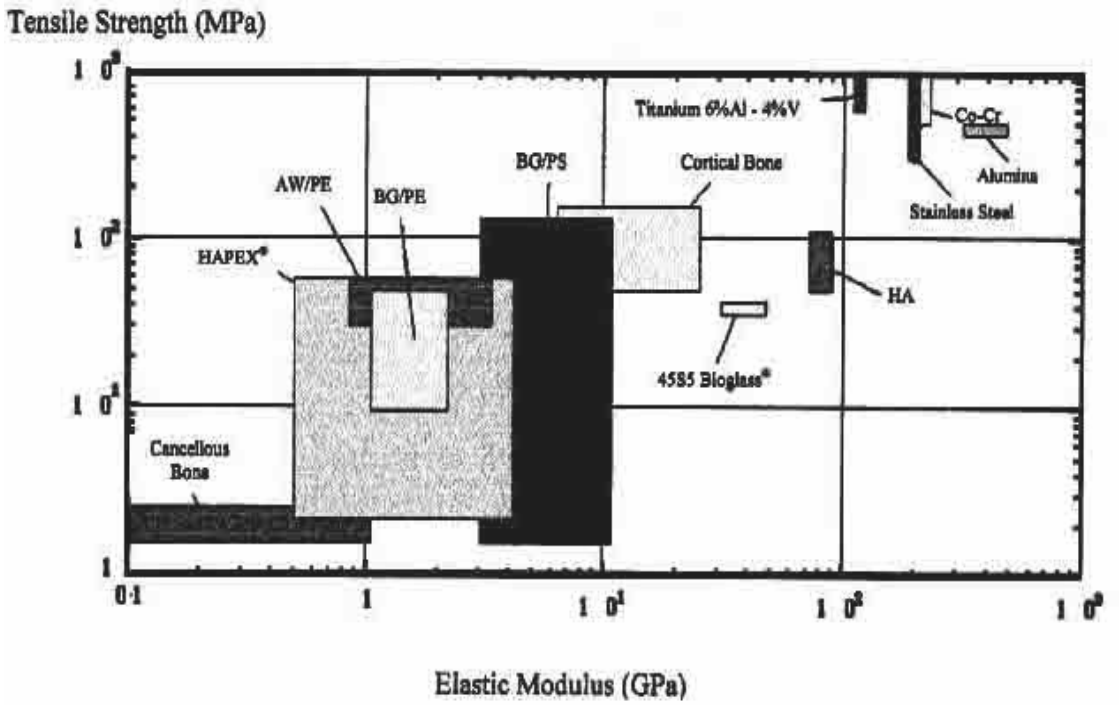

Figure 17. Comparison of the range of mechanical properties of various biomaterials with human bone (1).

Bending strength, compressive strength and tensile strength of dense HA ceramics are in the range of 38-250 Mpa, 120-900 MPa, and 38-300 MPa respectively. Strength decreases exponentially as the porosity increases. Young's modulus of HA is in the range of 35-120 GPa. It depends mostly on the measurement techniques, porosity and impurities. Vickers hardness is between 3,0-7,0 GPa (~600 HV). Wear resistance and friction coefficient of dense HA is comparable to that of human enamel (9,2).

4.5 HA Based Ceramic Composites

Research is concentrated on the preparation of composites due to the limitations originating from the poor mechanical properties of phase pure dense HA ceramics. In recent years many reinforcements, including particles (48,28), platelets (53), whiskers

(17,50,32), short fibers (46), PSZ (47,51), metal fibers and dispersoids (45) and nano-particles (22) have been used to improve the reliability of HA ceramics. The highest reported fracture toughness values were achieved by using 20-30% Fe-Cr alloy fibers with K_{IC} values of 6,0-7,4 MPa.$m^{1/2}$(2). Moreover in the case of other HA based composites fracture toughness values do not exceed the values of 1,4-3,9 MPa.$m^{1/2}$. The addition of most of these reinforcements into HA matrix may also cause a deterioration of biocompatibility and may promote the transformation of HA into TCP phase. The presence of TCP in the HA matrix may further cause enhanced bioresobability and slow crack growth susceptibility which consequently will deteriorate the mechanical properties and strength. Reinforcement of HA with bioinert materials in general will cause the preparation of a less bioactive material than HA.

Most of the reinforcements would increase the elastic modulus creating a mechanical system where most of the load is carried by the implant. Mismatch of the elastic modulus may cause the death of the natural bone tissue around the implant as discussed in the earlier sections. The preparation of dense HA based composites is usually harder by conventional sintering techniques which generates another significant disadvantage for the HA composite approach and may necessitate the use of most expensive formation/densification techniques such as HP, HIP must be used for the preparation of fully dense composites.

It's a fact that there is an authentic need for the preparation of highly biocompatible materials which can be used in load bearing applications such as artificial tooth roots or artificial bones. A new approach for the preparation of such a material is to use of completely biocompatible noncarciogenic HA whiskers as reinforcements in the HA matrix. The fracture toughness achieved is in the range of 1.4-2.0 MPa.$m^{1/2}$ (as compared with the 1.0 MPa.$m^{1/2}$ non-reinforced HA phase and 2.0 MPa.$m^{1/2}$ for the dense natural bone) (17). Compressive re-stressing and crack deflection are the main mechanisms, which may contribute to the improvement of fracture toughness. As mentioned above the main problem for process is the densification of such ceramics to theoretical value. Increasing the sintering temperatures above certain levels may cause the HA whiskers to transform into equiaxed larger grains (17) causing the loss of toughening effects due to the presence of whiskers. Expensive HP or HIP processing must be used to overcome these problems. It was recently reported that the whiskers fabricated by MSS route are stable up to 1300 ºC for 9 h without any degradation (32).

CHAPTER V

EXPERIMENTAL

5.1. Materials

Commercial HA and synthesized HA powders were used to investigate the densification behavior and mechanical properties of phase pure HA and HA whisker reinforced HA matrix composites. Properties of the commercial HA powder and the chemicals used to produce HA powders and whiskers are summarized in Table 8.

Table 8. Chemicals used for the processing of HA ceramics.

Name	Chemical formula	Properties
Hydroxyapatite (Aldrich)	$Ca_{10}(PO_4)_6(OH)_2$	FW=1004
Calcium nitrate (Sigma)	$Ca(NO_3)_2.4H_2O$	FW=236,2
Diamonium hydrogen phosphate (Merck)	$(NH_4)_2HPO_4$	FW= 132,6
Potasium sulphate (Sigma)	K_2SO_4	FW=174,3 99%
Ammonium hydroxide (Sigma)	NH_4OH	FW=35,05
Polyvinyl alcohol (Aldrich)	$[-CH_2CH(OH)-]_x^-$	Mw=9000-10000
	$[-CH_2CH(O_2CCH_3)-]_y^-$	

1.2. Methods

1.2.1. Synthesis and Characterization of HA powders

Stoichiometric amount of Ca and P were used for the preparation of HA powder by precipitation. HA powder was precipitated by the dropwise (10ml/min) addition of 0.1 M $(NH_4)_2HPO_4$ into 0.167M $Ca(NO_3)_2.4H_2O$ solution under constant stirring and the pH of the solution was continuously adjusted to 10 by the addition of NH_4OH and HNO_3 . The precipitate solution was further aged at ~60 ^oC over night. Precipitates were filtered by using a Buehler funnel and washed several times with deionized water in order to remove nitrate salts. The precipitate solution was ultrasonically treated about 15 minutes after it was resuspended during each wash. Precipitates were further washed with 96% ethanol to remove the excess water from the surface of the precipitate and to control the agglomeration state of the powders. The filtered precipitate cakes were further dried at 105 ^oC over night in ambient air.

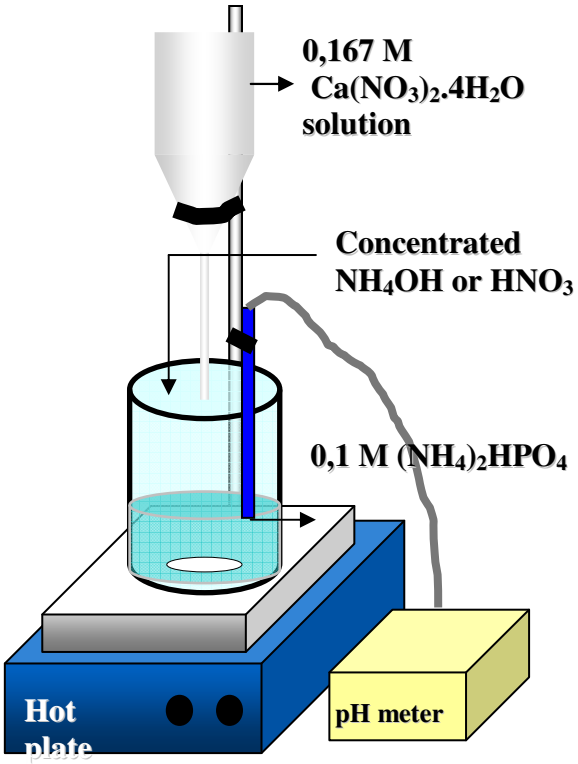

Figure 18. Schematic drawing of experimental set-up used for powder precipitation.

The effects of the precipitation conditions on the powder properties were investigated by conducting 12 different precipitations. Six different precipitations were conducted at pH levels of 4, 6, 8, 9, 10, and 11 in order to investigate the effects of pH on powder characteristics while aging time and temperature were kept constant. The effects of aging temperature were investigated in the 30-90 ºC range while the pH and the aging time were kept constant at 10 and 24 hrs respectively. Effect of aging time was investigated by keeping the pH constant at 10 and at 60 ºC aging temperature while precipitates were aged for 0, 0.5, 1, and 48 hours. All of the oven dried precipitates were heat treated at 300, 400, 500, 800, and 1250 ºC in order to investigate the thermal stability and phase structure development in the powders.

A final set of precipitations were conducted at pH=10, 60ºC and aged for 24 hours, where initial Ca/P ratio was adjusted to 1,5 and 1,667 respectively in order to investigate the effects of initial reactant concentrations. These oven-dried powders were calcined at 1000, and 1250 ºC for phase structure development analysis.

The characterization of the powders was performed with the following techniques: XRD analyses were performed in order to investigate the crystallographic structure. Optical (OLYMPUS BX60M) and SEM (Philips XL30S FEG) microscopy observations were performed for morphology and particle size determinations. Sedigraph (Micromeritics Sedigraph 5100) and Zetasizer (Malvern 3000 HS) were used for particle size distribution determinations.

1.2.2. Synthesis and Characterization of HA whiskers

Hydrothermal synthesis and molten salt synthesis methods were used for the preparation of HA whiskers. For the hydrothermal synthesis of HA whiskers, 50cc of 0,4 M $Ca(NO_3)_2.4H_2O$, 100cc of 0,6 M $(NH_4)_2HPO_4$, and 50cc of 0,42 M EDTA solutions were used. $Ca(NO_3)_2.4H_2O$ and EDTA solutions were reacted to get the CaEDTA solution in the first step of synthesis. $(NH_4)_2HPO_4$ and CaEDTA solutions were then mixed and the pH was adjusted with concentrated NH_4OH. The prepared clear solution was poured into a teflon beaker and placed in a stainless steel reactor to perform the hydrothermal synthesis. The closed reactor was heated to temperatures in the 150-225^{0}C range in a sand bath for 1 hour with continuous stirring and was cooled down to room temperature rapidly in an ice bath at the end of the period. Precipitated

whiskers were washed with deionized water and oven dried at 105 ºC.A photograph of the hydrothermal whisker synthesis set-up is shown in Figure 19.

Figure 19. Photograph of the experimental setup used for the hydrothermal synthesis of whiskers.

MSS whiskers were prepared from a mixture of commercial HA powder and potassium sulfate (K_2SO_4) which were thoroughly mixed in an aqueous medium which was accomplished by dissolving the salt in water and subsequent addition of the HA powder to this salt solution. This suspension was further dried in an oven at 100^0C. Powder to salt weight ratio was set at 3. The mixture of salt and HA powder was then put into an alumina crucible and heated up to 1100ºC (melting point of K_2SO_4 is 1060ºC) with 4ºC/min heating rate. The mixture was kept at this temperature for 1h to achieve the complete dissolution of HA powder by the flux and growth of the whiskers and then cooled down to room temperature with 20 ºC/ min cooling rate. The heat treated solid mass was washed with deionized water for several times for the recovery of potassium sulfate free HA whiskers. These whiskers were characterized with similar HA powder characterization techniques mentioned above.

1.2.3. Preparation of Composite Powders

Both commercial and precipitated powders were mixed with 10-30 vol % HA whiskers to prepare the composite powder mixtures. Suspensions of HA powders with high solids contents were prepared and treated in an ultrasonic bath for 10 minutes to obtain well dispersed HA suspension. Predetermined amounts of whiskers were added into these suspensions and ultrasonic treatment was performed again to get the homogeneous dispersion of whiskers under constant stirring. 3w/w% PVA was added to these suspensions as a binder. These suspensions were further dried to about 6w/w% water content in an oven at 105 ºC. Suspensions were stirred periodically during drying in order to prevent segregation of whiskers.

1.2.4. Sintering Studies and Characterization

Powders with 3w/w % PVA and 6w/w % water were compacted in a stainless steel die 1cm in diameter under 160 MPa pressure to about ~55% of theoretical density (3.16 g/cm^3). Five pellets were prepared to investigate the densification behavior and mechanical properties (3 for density measurements and 2 for mechanical testing) for each run. These pellets were sintered at 800, 900, 1000, 1050, 1100, 1150, 1200, 1250, 1300 ^{0}C for 2 hours with 4 ºC/min in a high temperature furnace (Carbolite RHF 1600) then cooled to room temperature in the furnace in order to investigate the densification behavior of the pure HA and composite compacts. The densities of 3 sintered pellets were measured by using Archimede's density measurement kit (Sartorious BP 2105). Optical microscopy (OLYMPUS BX60M) and SEM (Philips XL30 SFEG) observations were performed for microstructure investigation.

1.2.5. Mechanical Testing

Vickers hardness indentation method (HVS-1000) was performed by at least 3 indentations for each pellet to get the Hv results. 9.8070 N load was applied for 20 s to Vickers indenter. Compression tests were conducted by Testometric AX500-100 universal testing machine to obtain compressive strength and elastic modulus of the sintered samples. Planar surfaces of the samples were polished with 1-micron diamond solution to obtain smooth surfaces.

CHAPTER VI

RESULTS AND DISCUSSION

The results of powder and composite preparation studies will be discussed in the following order in this chapter: i) powder preparation and characterization ii) composite preparation and characterization.

6.1. Synthesis of Hydroxyapatite

6.1.1.Powder preparation

6.1.1.1. Effects of initial Ca/P ratio.

The initial Ca/P ratio was adjusted to 1.5 and the stoichiometric value of 1.66 during precipitation and its effects on the properties of the HA powders was investigated. XRD analysis results showed that an initial stoichiometric amount of Ca and P in the precipitation environment generates amorphous HA phase in the as precipitated oven dried powders. On the contrary to this structure a very crystalline mixture of other calcium phosphate phases were detected in the as precipitated oven dried powder prepared with an initial Ca/P ratio of 1.5 in terms of the reactants introduced in to the precipitation medium as can be clearly seen from the XRD patterns presented in Figure 20. These findings indicate the presence of a delicate phase equilibrium between a series of calcium phosphate phases at pH=10 which may shift towards more crystalline phases from an amorphous phase pure HA as Ca ion deficiency increases in the system. This may also have significant effects on the nucleation and crystal growth processes for various phases present in the system which was not affected deeply by the 24 hours aging .

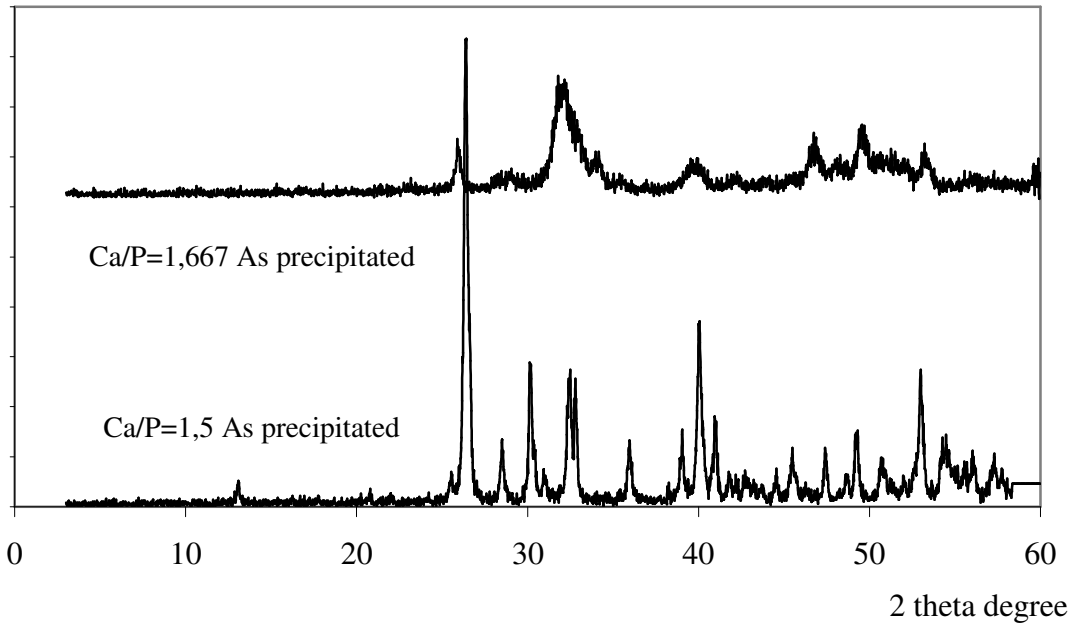

Figure 20. XRD patterns of the precipitated powders with two different initial Ca/P ratios.

After heat treatment at 1000 ºC while stoichiometric powder transforms into a crystalline hydroxyapatite, Ca deficient precipitates decompose into a complex mixture of other Ca deficient forms, TCP and monetite as presented in the XRD patterns given in Figure 21. The phase equilibrium present in the as precipitated powders seems to persist at this calcinations temperature.

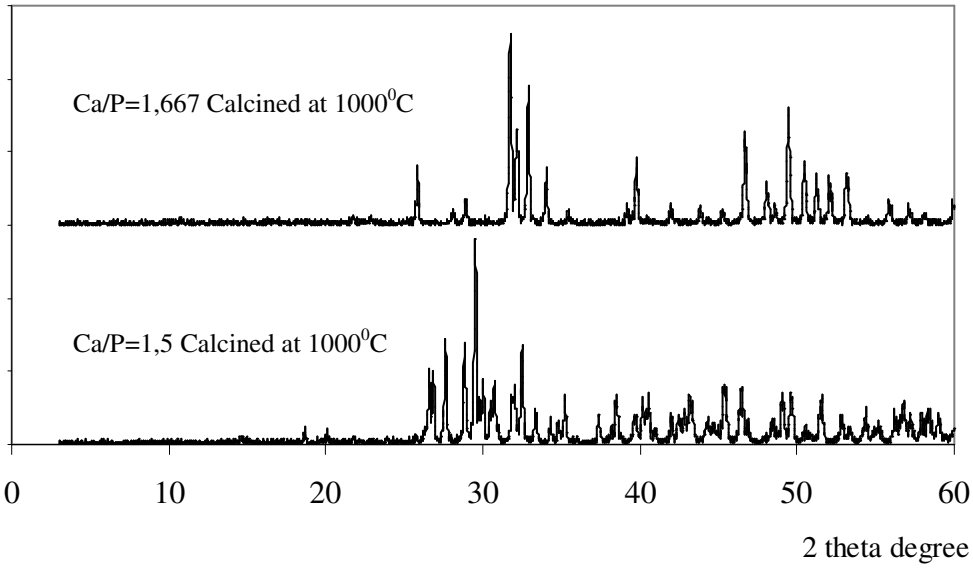

Figure 21. XRD patterns of the powders heat treated at 1000 ºC with two different initial Ca/P ratios.

6.1.1.2. Effects of pH

As mentioned above in previous chapters, OH^- ion concentration in the precipitation medium is one of the most important parameters on the hydroxyapatite formation. The pH of the starting solutions can affect the precipitation by altering the solubility of the phases and further affect powder agglomeration state of the powder. The variation of the solubilities of different phases present in the precipitation medium as pH incresases may change the phase structure and the stoichiometry of the forming phases. Recovered amount of precipitates as a function of pH given in Figure 22 have shown that the precipitate weight increases with increasing pH. Recovered precipitate yields at pH 9 and 10 were very close to the theoretical HA precipitate yield which is 8.17 g per precipitation batch assuming complete Ca conversion to HA. Powder recoveries above this theoretical amount may be due to the presence of adsorbed water layers on the surface of the powders at pH 10 and 11.

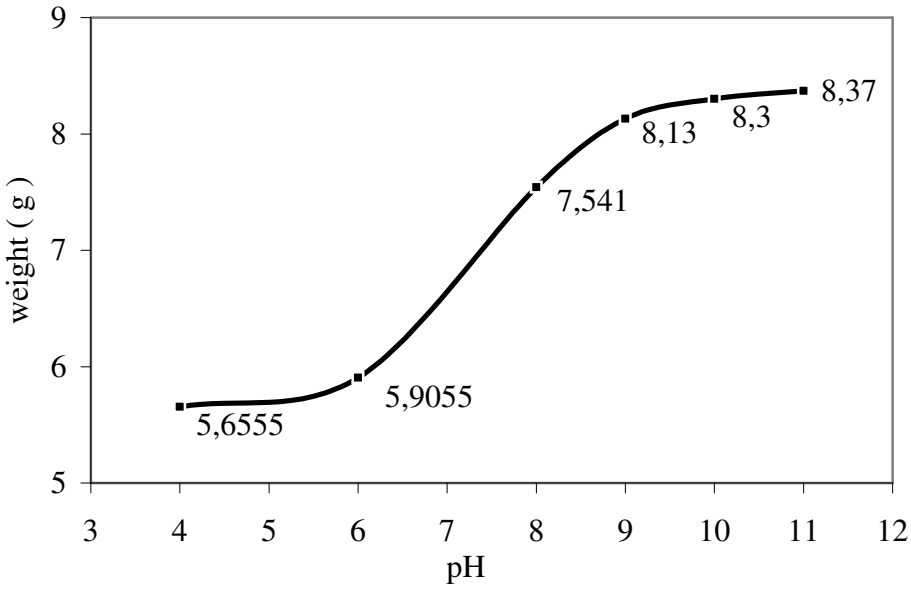

Figure 22. Precipitate weight of the powders precipitated at different pHs

The XRD patterns given in Figure 23 indicate that the formation of HA starts over pH 8. Below this pH other compounds form which exist in the Ca-P-H2O system. Highly crystalline plate like agglomerated most likely monetite / brushite crystals were obtained. These crystallites have approximately 500nm thickness and 5x3 micrometer

surface dimensions as seen in the SEM micrograph given in Figure 25. Mainly Brushite phase was detected at pH 6 from the XRD pattern given in Figure 23. These perfectly dispersed rectangular-prism brushite crystals have approximately 6x4x1 micrometer dimensions as given in Figure 26 with sharp intense X-Ray peaks given in Figure 23. As mentioned before hydroxyapatite formation is starts over pH 8. At this pH characteristic peaks of the HA start to appear in the XRD pattern and as the pH continues to increase pure HA peaks become more distinct with the sharpest HA peaks detected at pH 9. The morphologies of the crystallites begin to alter when compared with the precipitates produced in acidic medium above pH 8. This morphological transformation can be explained by the kinetics of precipitation. As the OH^- concentration increases solubility of the precipitate decreases causing more stable nuclei formation during crystallization, which cannot redissolve in the precipitation medium.

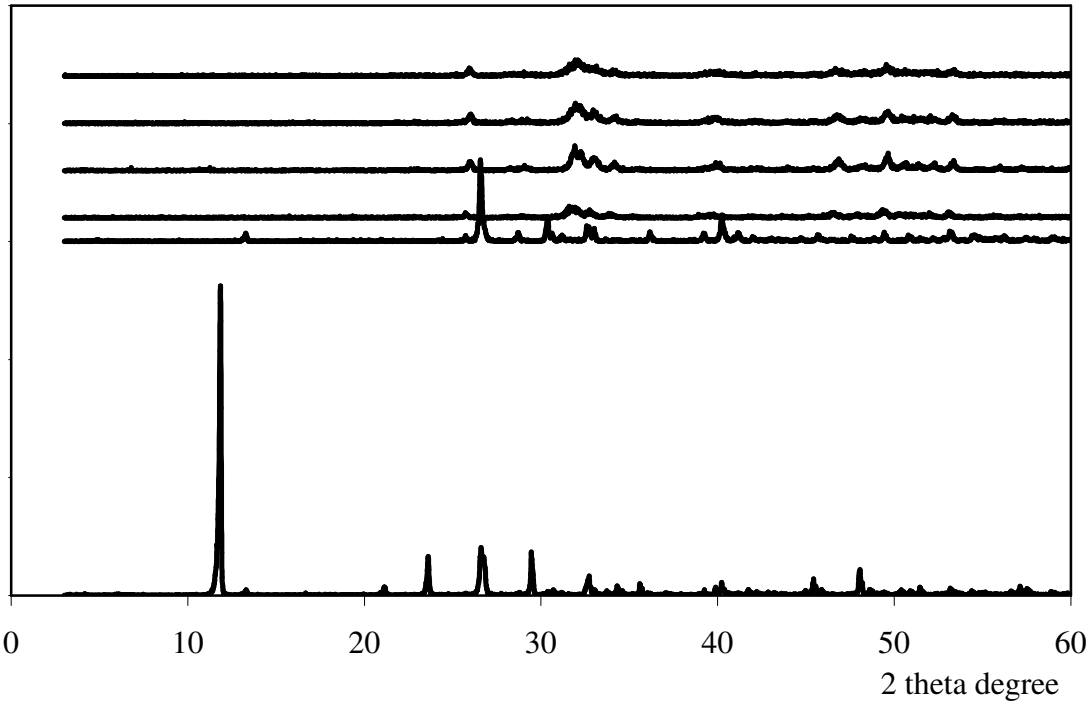

Figure 23. XRD patterns of the precipitated powders at pH 4,6,8,9,10,11 from bottom of the figure to the top respectively.

As mentioned in the experimental section Ca was slowly introduced to the precipitation medium by drop wise addition (10ml/min) in order to control the nucleation and growth rate. Figure 24 shows that there is no significant difference in the crystallite size of the as precipitated powders which is calculated by Sherer equation from XRD pattern using the single peak at 25.8 2Θ degree of the precipitates obtained

at different pH. After heat treatment at different temperatures up to 1250 ºC there is an increase in crystallite sizes from ~30nm to 40-90 nm ranges was observed as expected. The increase in the crystallite size with temperature up to 1250 ^{o}C ia inversely proportional with pH. Only the behavior of the pH 8 powder deviates from this observation this may be explained by the decomposition of HA into other phases because of initial nonstoichiometry and / or impurity phases.

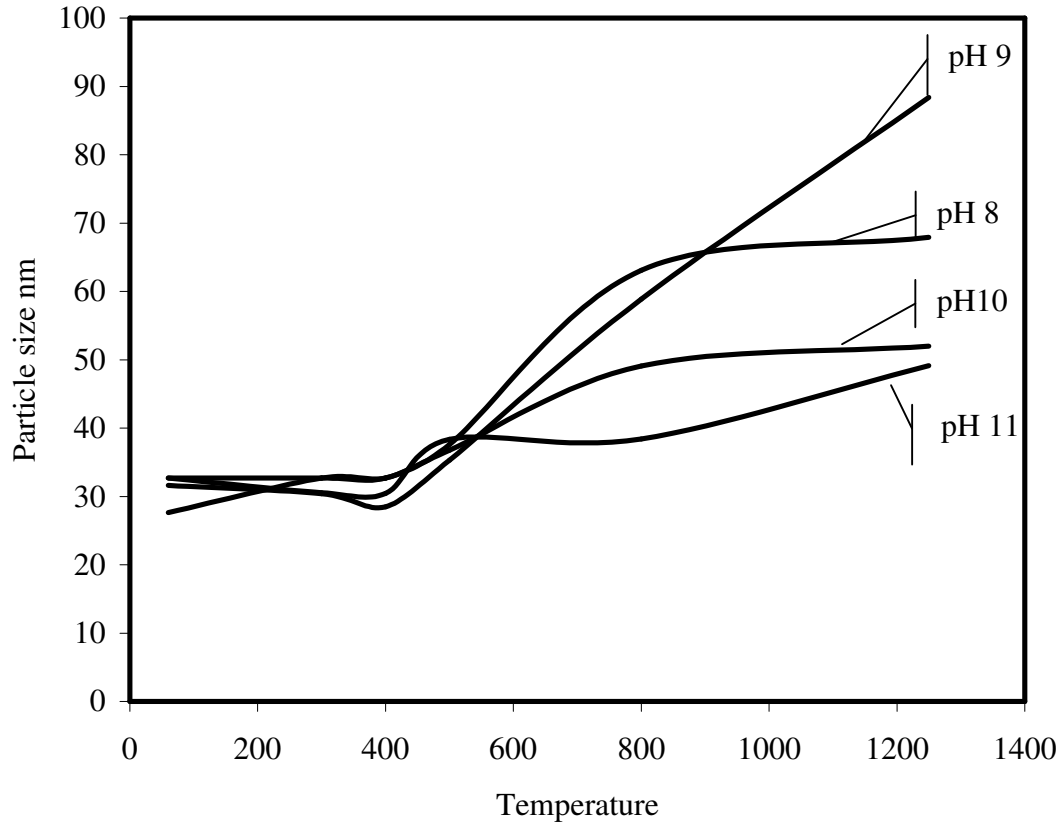

Figure 24. Change in the crystal size of the powders precipitated at different pH with temperature

SEM micrographs given in Figures 25 through 30 verified the notable morphological changes mentioned previously. Phase evolution studies reveal that formation of stable HA phase at 1250 ºC, well known sintering temperature for HA, is mostly possible in precipitations conducted over pH 10, at 60 ºC aging temperature and 24 hrs aging time. At pH 9 and 8 partial decomposition of HA into an Alpha-TCP (Ca/P= 1.5) phase was detected (detection limit of XRD for impurity phases >5%) (Figure 31).

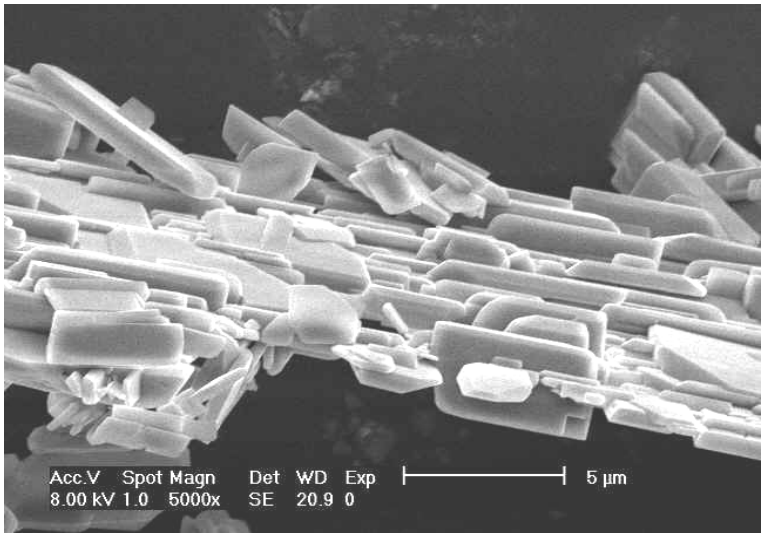

Figure 25. SEM micrograph of the powder precipitated at pH 4.

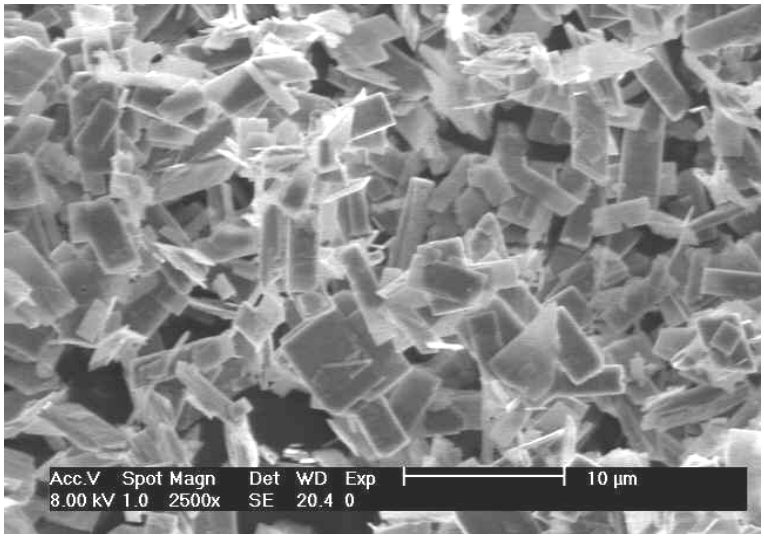

Figure 26. SEM micrograph of the powder precipitated at pH 6.

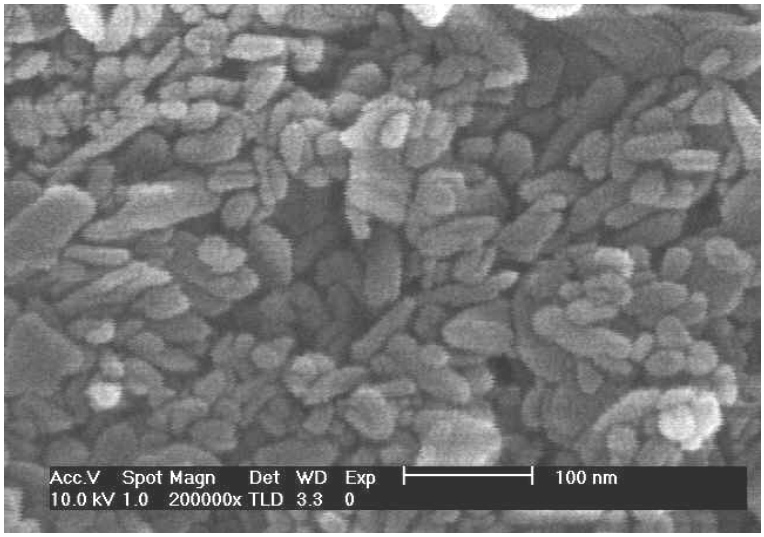

Figure 27. SEM micrograph of the powder precipitated at pH 8.

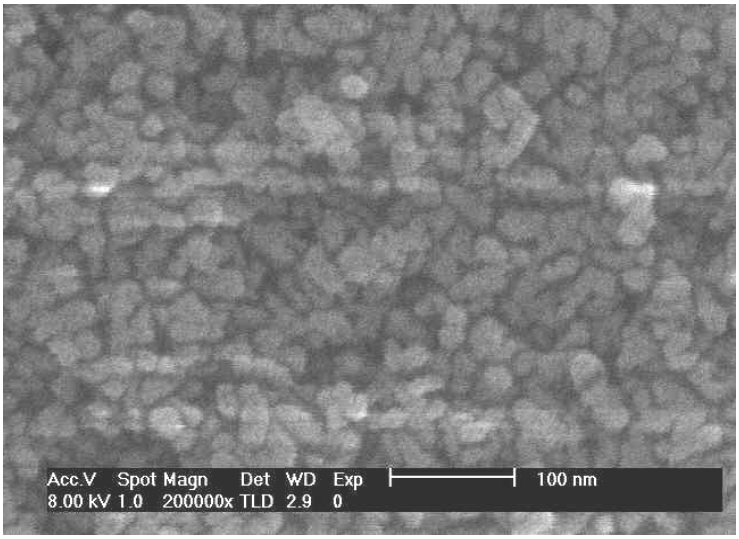

Figure 28. SEM micrograph of the powder precipitated at pH 9.

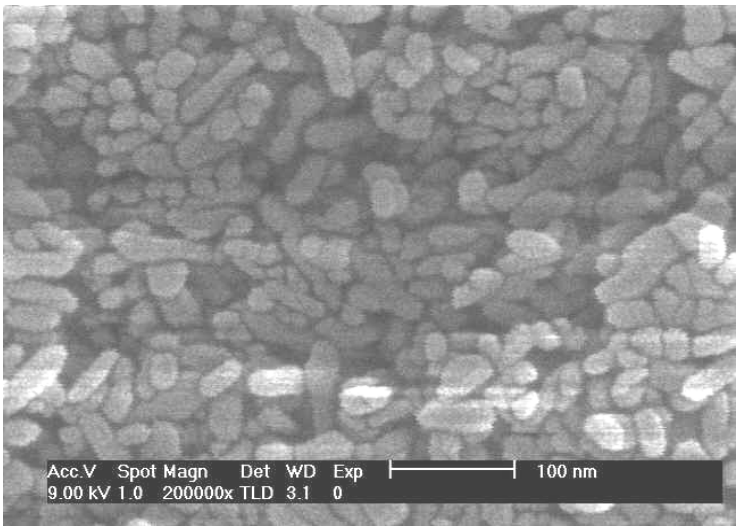

Figure 29. SEM micrograph of the powder precipitated at pH 10.

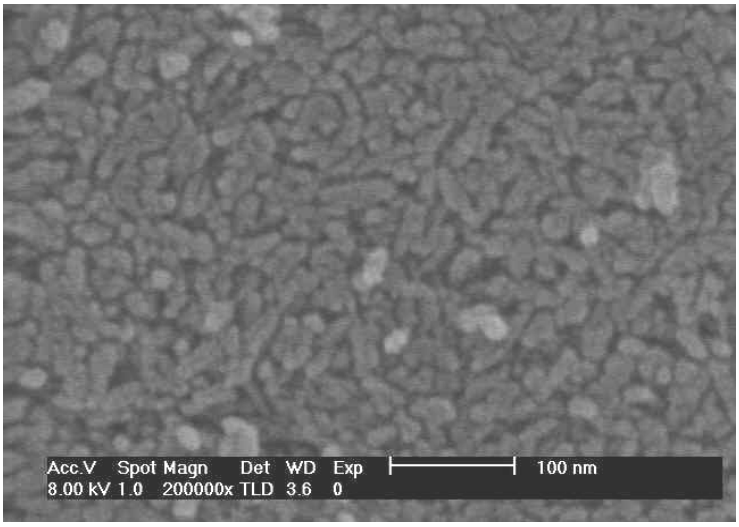

Figure 30. SEM micrograph of the powder precipitated at pH 11.

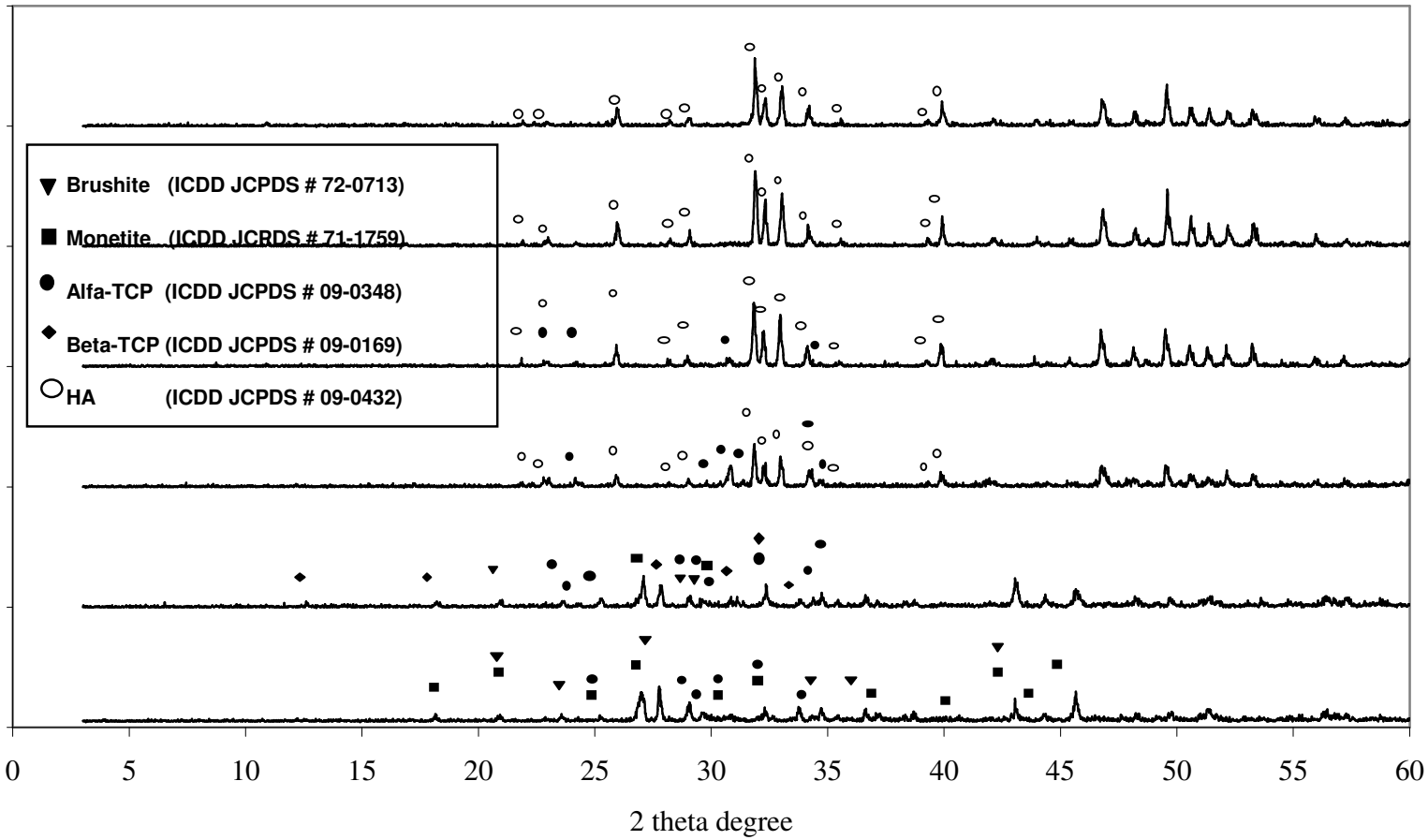

Figure 31. XRD patterns of the powders precipitated at pH 4, 6, 8, 9, 10, 11 after heat treatment at 1250 ^{o}C.

6.1.1.3. Effects of aging temperature

Two identical precipitates were prepared at pH10 and aged at 30 and 90 ºC for 24 hrs in order to investigate effects of aging temperature on powder characteristics. Both powders displayed characteristic HA peaks as seen from Figure 32. The sharper peaks detected in XRD pattern of the 90 ºC aged powder indicates a better crystallinity compared to 30 ºC with aged powder. Increasing aging temperature increases the dissolution-recrystallization kinetic in the system. As a result, the powder aged at 90 ºC displayed better crystallinity and larger crystallite size as shown in Figure 33. Although increasing aging temperature leads to the formation of relatively larger crystallite sizes approximately 35nm at room temperature, phase evolution studies with heat treatment temperature showed that there was no decomposition at 1250 ºC into other phases unlike powder aged at 30 ºC which is shown in Figure 36. The preferred orientation for HA is along the <002> direction as mentioned earlier. Since increasing temperature increases the crystallinity, crystallite size increases with aging temperature as seen from Figures 34 and 35. Heat treatment studies indicated that aging at 90 ºC leads to the formation of a more stable phase at 1250 ºC whereas 30 ºC powder results in an unstable form of HA and this powder partially decomposed into Alpha-TCP phase as shown in Figure 36.

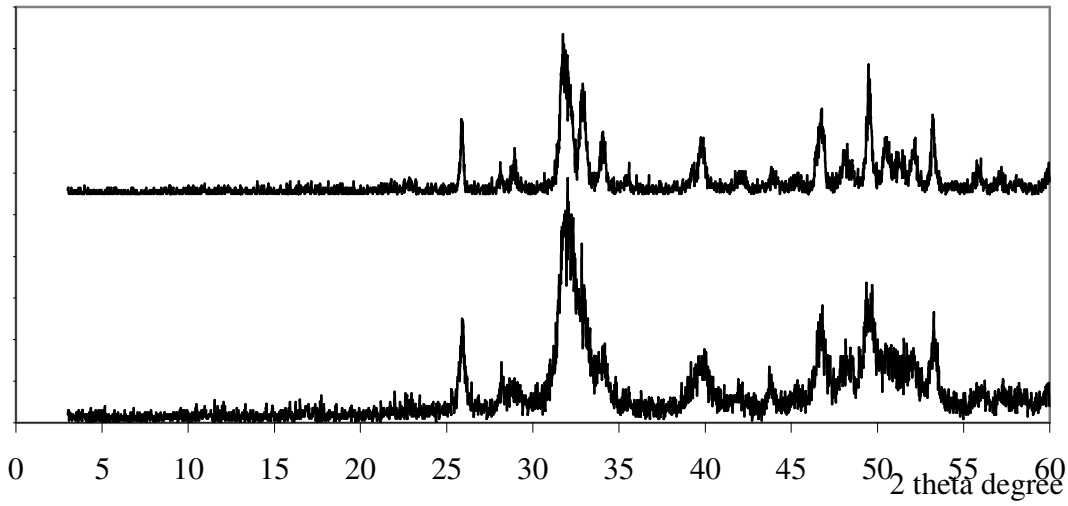

Figure 32. XRD patterns of the precipitated powders at ph 10 aged at 30,90 ^{o}C for 24 hrs.

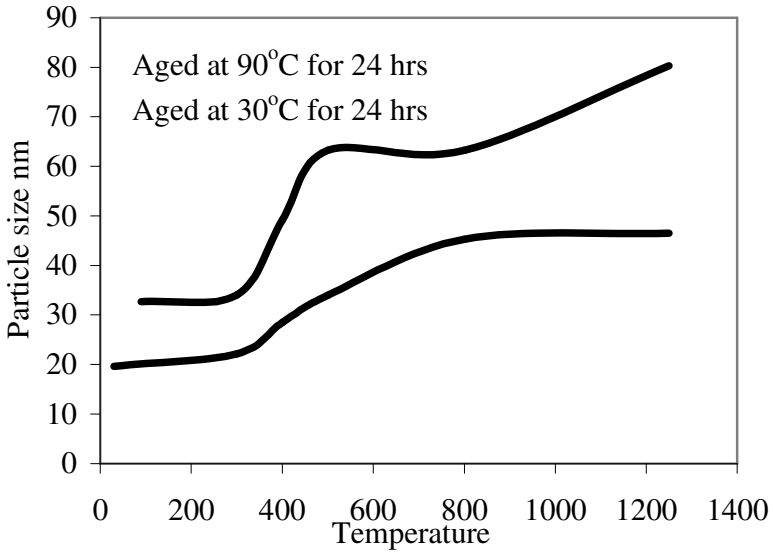

Figure 33. Change in the crystal size of the powders aged at 30,90^{0}C for 24 hrs with respect to temperature.

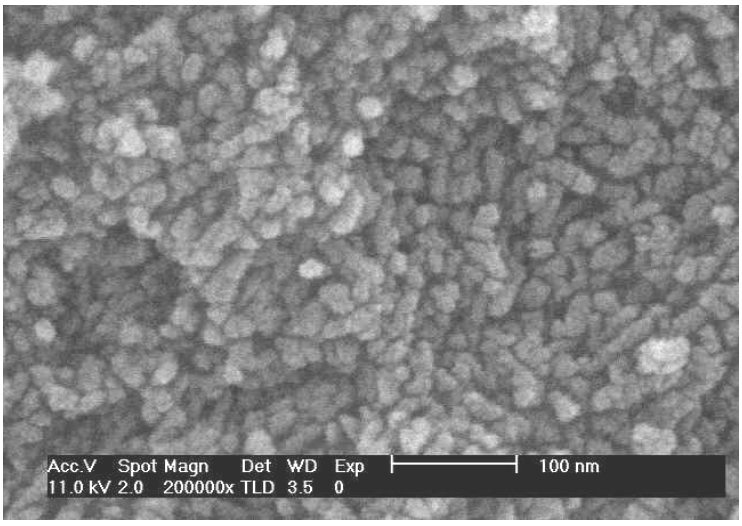

Figure 34. SEM micrograph of the powder aged at 30 ^{o}C.

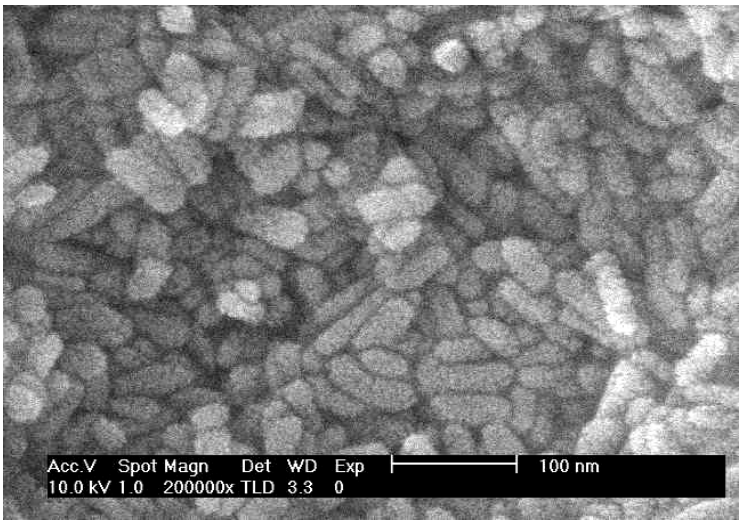

Figure 35. SEM micrograph of the powder aged at 90 ^{o}C.

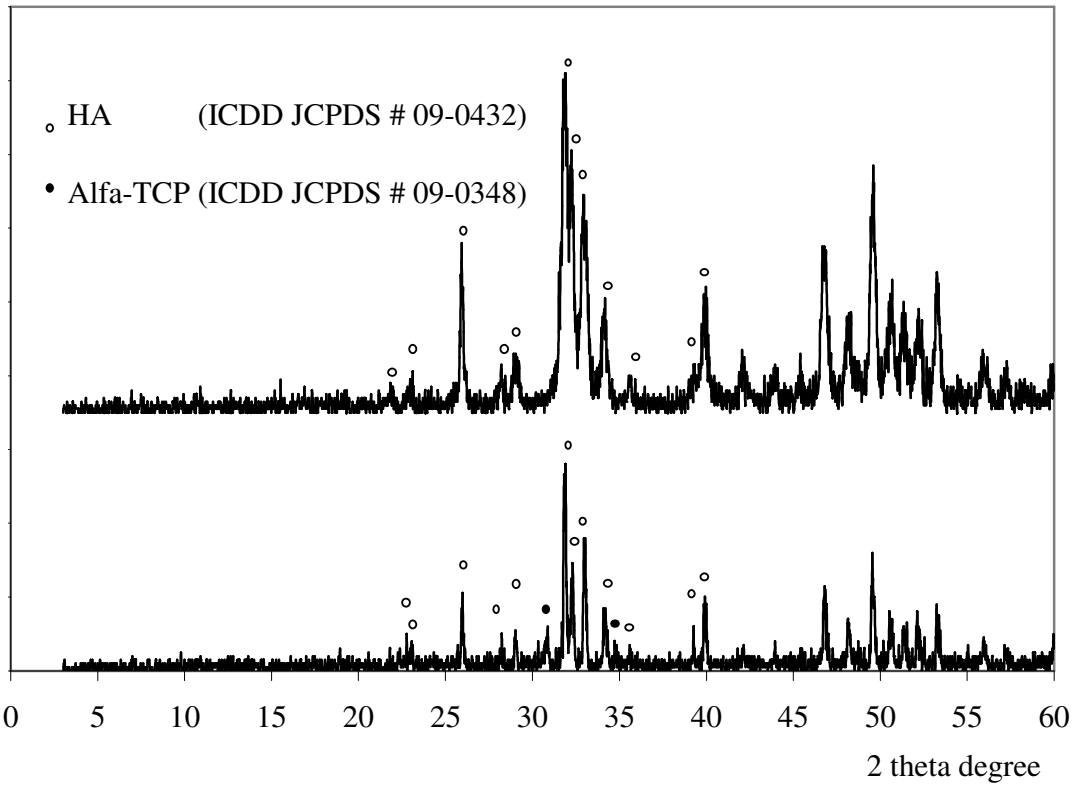

Figure 36. XRD pattrens of the aged powders after heat treatment at 1250 ^{o}C.

6.1.1.4. Effects of aging time

Another important parameter for the precipitation of HA is aging time. Increasing the aging time theoretically supplies the necessary time for the crystallites to rearrange. As seen from Figure 37 all the powders aged for different periods displayed characteristic HA peaks and no significant differences can be observed either in intensity or sharpness. There are slight differences in crystallite sizes at room temperature and after heat treatment as shown in Figure 38. SEM micrographs given in Figures 39, 40, 41, and 42 indicate that aging time has no effect on the morphology or crystallite size of the precipitates but the size distribution becomes narrower. The only 1250 ºC stable pure HA phase was obtained from the 48 hrs aged precipitate. All other precipitates partially decomposed into Alpha-TCP phase at that temperature as is apparent from the XRD patterns given in Figure 43.

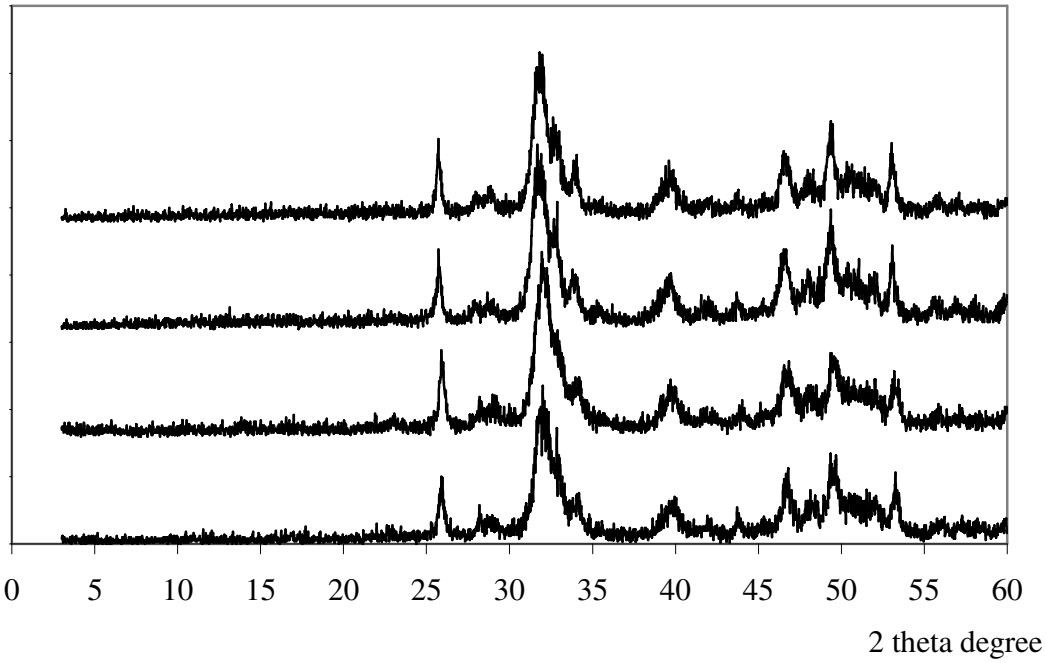

Figure 37. XRD patterns of the aged precipitated powders at pH 10 and 60^0C for various periods. 0, 0.5, 1, 48 hours from bottom to top of figure.

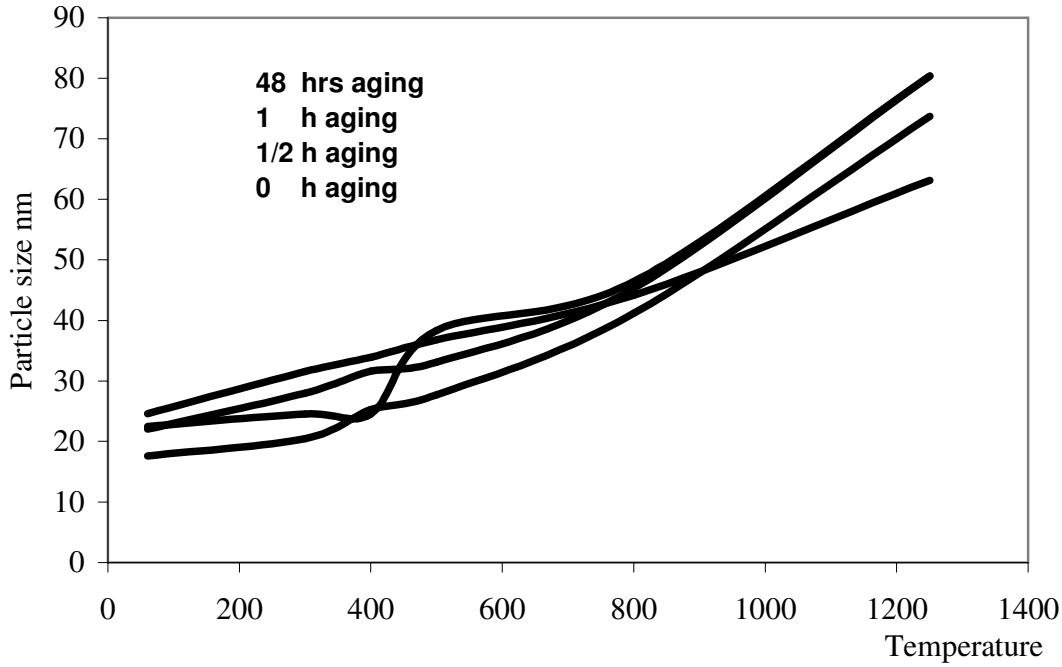

Figure 38. Change in the crystal size of the powders aged for 0, 1/2, 1, 48 hours at pH10 and 60 ^{o}C with temperature.

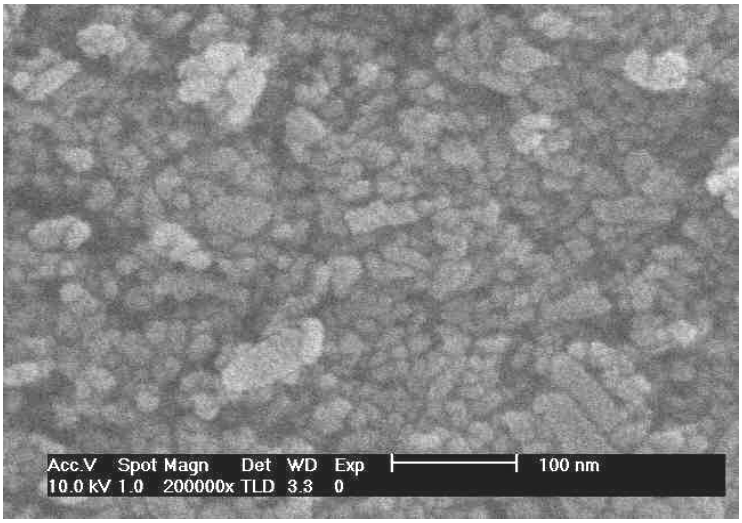

Figure 39. SEM micrograph of the powder precipitated at pH10 at 60 ^{o}C without aging.

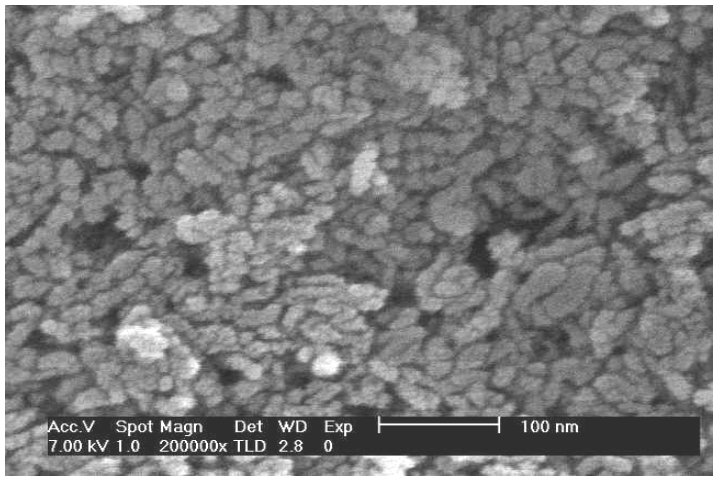

Figure 40. SEM micrograph of the powder precipitated at pH10 at 60 ^{o}C aged for ½ h.

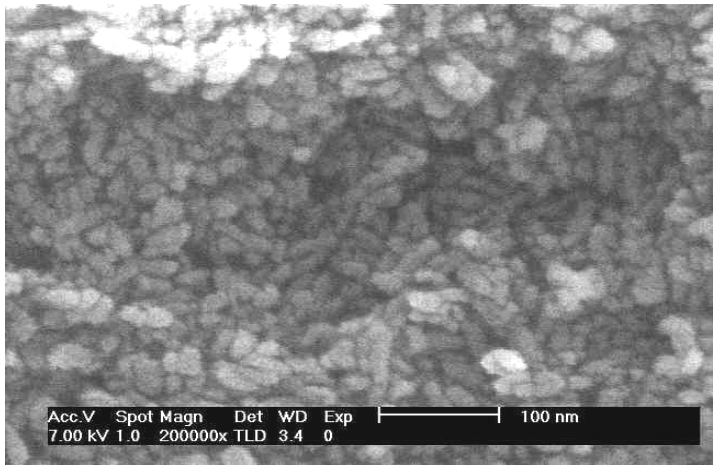

Figure 41. SEM micrograph of the powder precipitated at pH10 at 60 ^{o}C aged for 1 h.

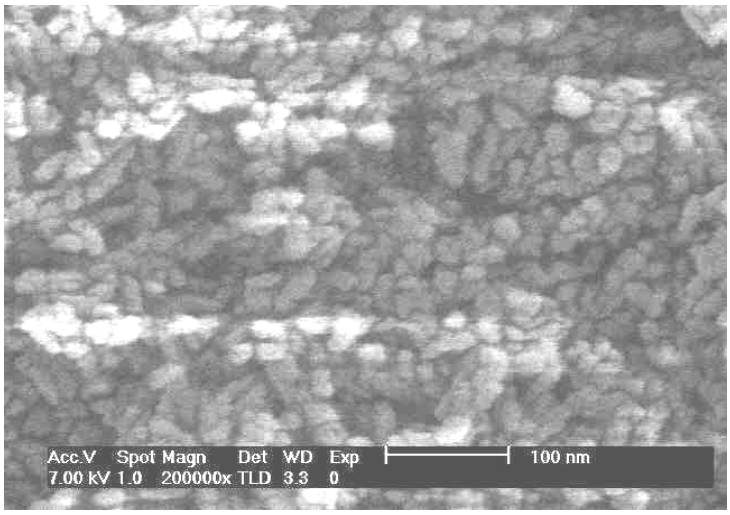

Figure 42. SEM micrograph of the powder precipitated at pH10 at 60 ^{o}C aged for 48 h.

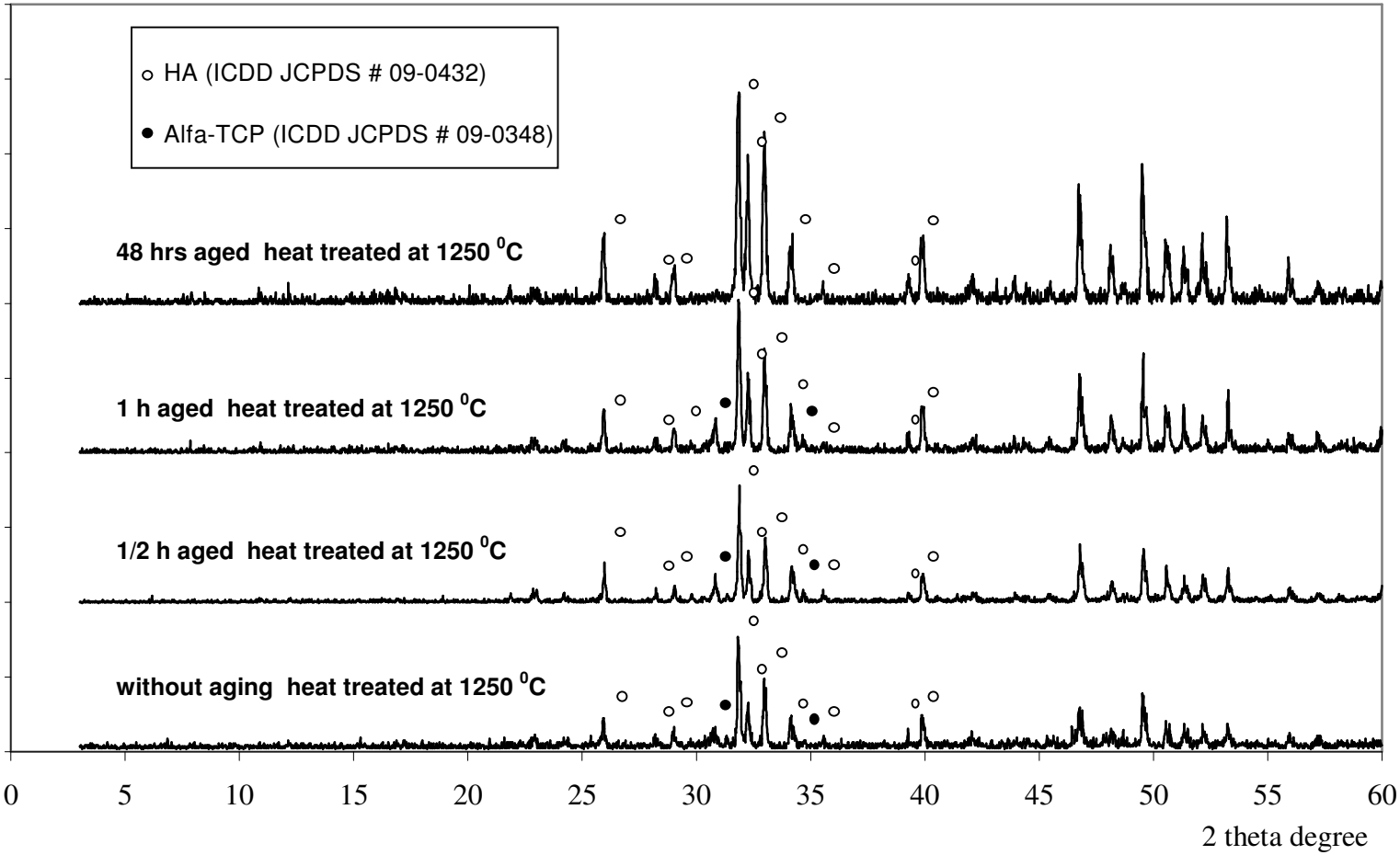

Figure43. XRD pattrens of the aged powders at 60^0C and pH10 after heat treatment at 1250^0C.

6.1.2.Whisker preparation

In this study two different methods were used to prepare HA whiskers. First one is the hydrothermal method and the second one is molten salt synthesis method. The principle of hydrothermal synthesis is based on a slow release of one of components of a compound to achieve homogeneous nucleation-crystallization. On the other hand, in molten salt synthesis the process is based on the dissolution-recrystallization of a compound in a proper flux.

6.1.2.1. Hydrothermal synthesis of HA whiskers (HDT)

Theoretical amount of Ca and 3 times that of P were used in the synthesis. The slow release of Ca ions into the syntesis medium, Ca ions were bound to a compound that decomposes slowly under hydrothermal conditions. Ca and P sources were then mixed together and sealed in a closed stainless steel container. This system was heated up to temperatures 150-225 ºC in order to investigate the extent of reaction-temperature relationship. The weight of the precipitated whiskers increase significantly with increasing temperature and theoretical amount of precipitate was obtained at 225 ºC as seen in Figure 44. Similar significant changes were not observed in the morphology of the whisker with increasing temperature. SEM micrograph of the hydrothermally synthesised whiskers displays that almost hexagonal needle like HA whiskers ,~20micrometer in length and ~1-2 micrometer in diameter, with an aspect ratio of ~10 was obtained at 225 ºC as shown in Figure 45. XRD pattern of the whisker given in Figure 46 displayed sharper and more intense peaks when compared with the peaks of the precipitated powders. This indicates the high crystallinity and prefered orientation of the whiskers. In addition, differences in the intensity ratios between the peaks (300)/(211) and (002)/(211) when compared to that of the powders indicate that the elongation direction of the whiskers is along the crystallographic c-axis [001] (25).

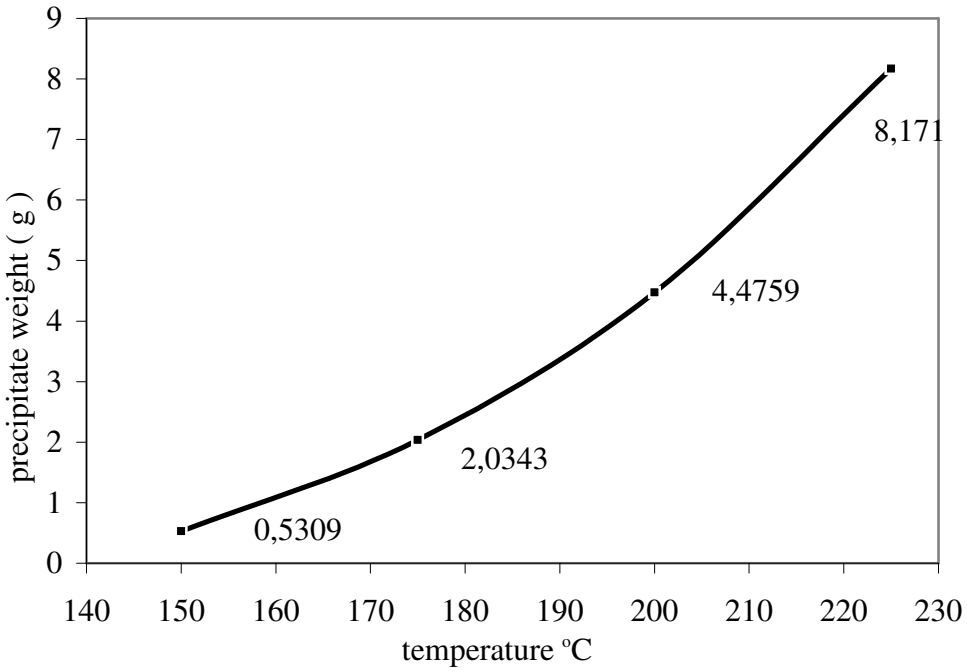

Figure 44. Precipitate weight of the whiskers precipitated at different temperatures

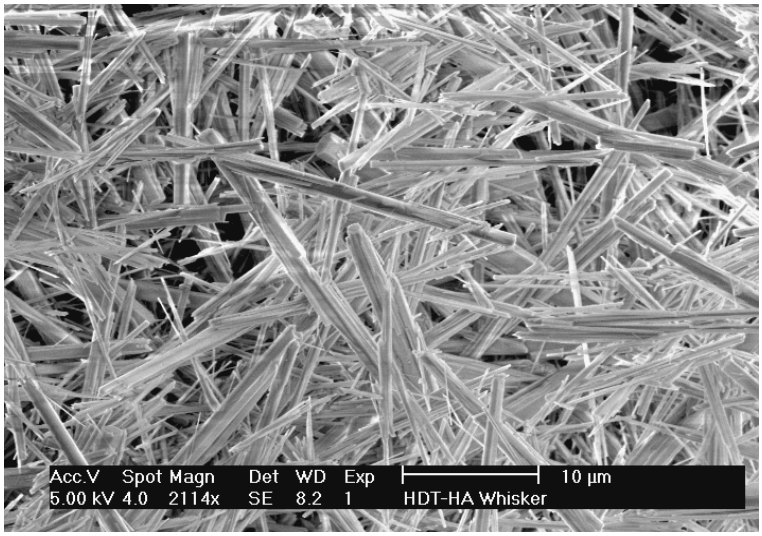

Figure 45. SEM micrograph of the hydrothermaly synthesized whiskers

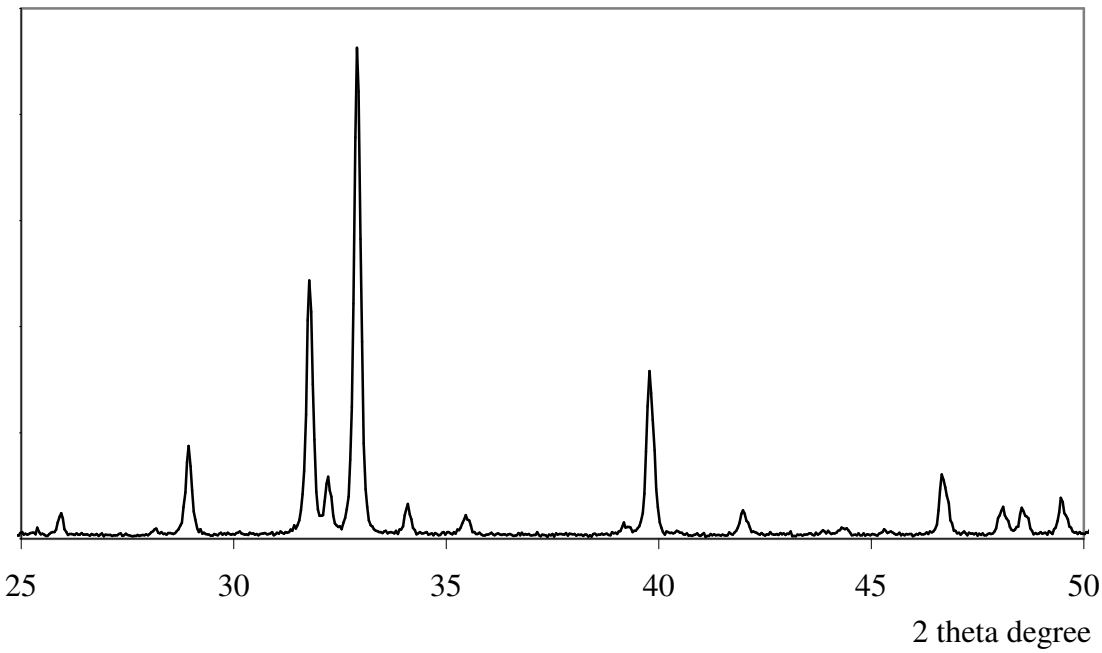

Figure 46. XRD pattern of the hydrothermaly synthesised whiskers

6.1.2.2. Molten salt synthesis of HA whiskers (MSS)

The principle of this method is based on a dissolution-recrystallization process of HA in a proper flux. As mentioned in experimental chapter K_2SO_4 was used as a flux. Optical microscope observations reveal that monodispersed, transparent, hexagonal and rodlike HA whisker was produced as shown in Figures 47,49. SEM micrographs given in Figure 48 displays that dimensions of the whiskers vary between 10-20 micron in length and 1-5 micron in diameter with an aspect ratio of 5-15. On the other hand, some spherical particles ~2-3vol % was observed in recovered whisker batchs. HA/ salt ratios were changed between 1-3 in order to eliminate these spherical particles. However SEM and optical microscope observations indicated that there is no direct relationship between the existance of those particles and the HA/salt ratio. Presence of those particles may be related with the synthesis temperature and or heterogeneous mixing of salt and HA powder (32). A representative wisker HA XRD pattern is given in Figure 50, but as mentioned in previously the most intense peak was obtained from (300) plane related with the preferential growth of whiskers along the c-axis.

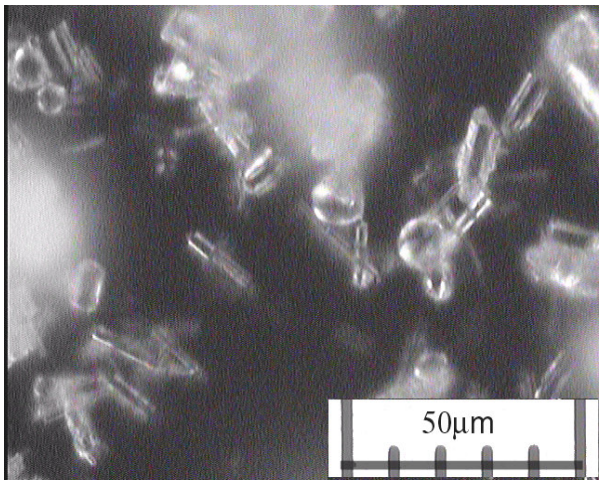

Figure 47. Optical microscope image of the MSS whiskers showing the spherical particles.

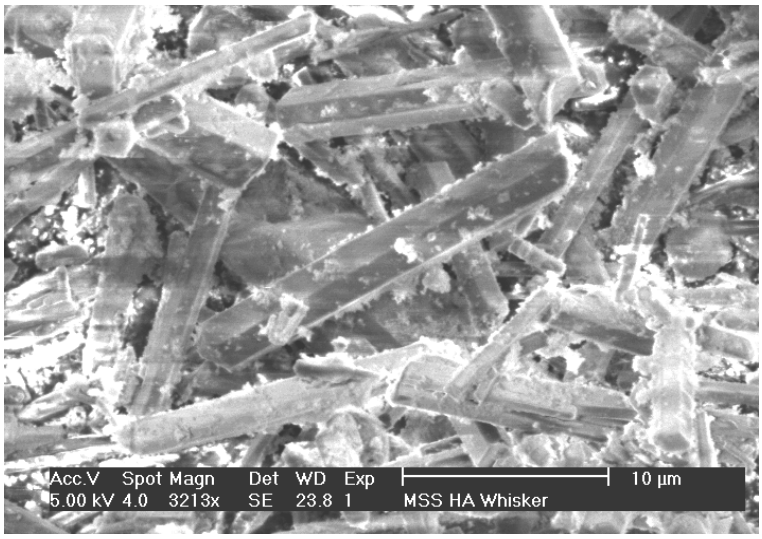

Figure 48. SEM micrograph of the MSS whiskers.

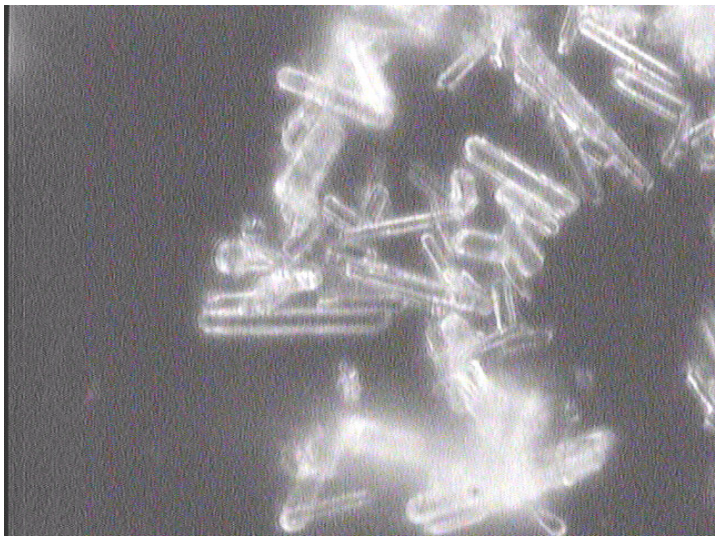

Figure 49. Optical microscope image of MSS whiskers.

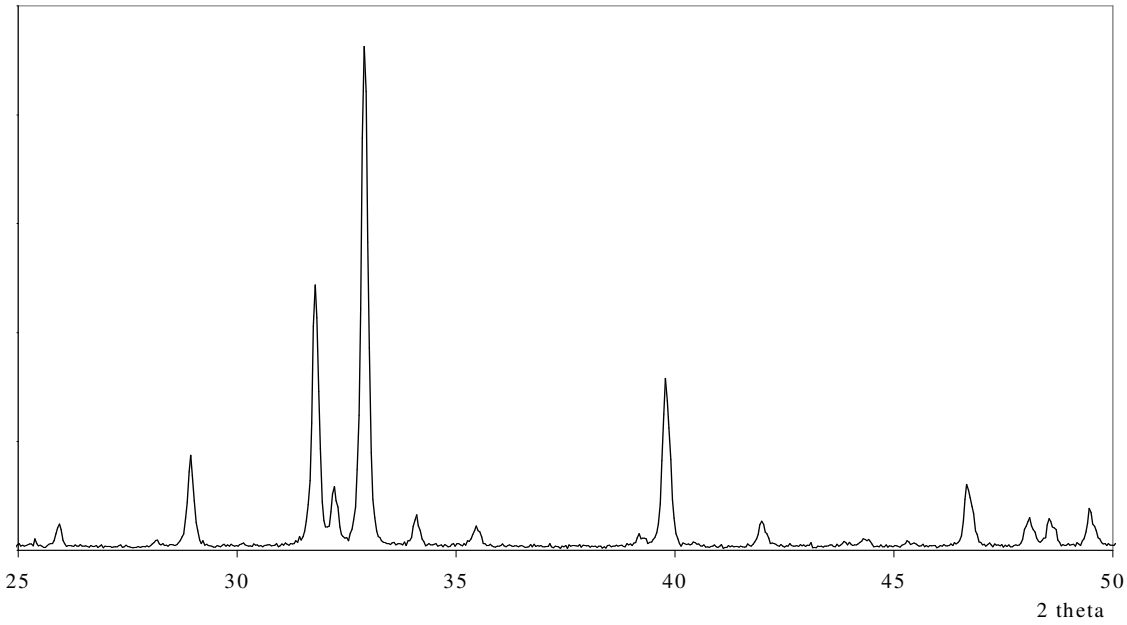

Figure 50. XRD pattern of the MSS whiskers**.**

6.2. Composite Preparation

In this study commercial and synthesised HA powders were used to prepare the HA whisker reinforced HA composites. The powder preparation results discussed above indicated that pH=10, 60 ºC aging temperature and 24 hrs aging time as the optimum powder preparation conditions where nearly equaxed 40-60 nm size HA particles as seen in Figure 51 with maximum yield can be obtained. As seen from Figure 52, that powder displayed characteristic pure HA peaks corresponding with the peaks given in JCPDS # 09-0432. Oven dried precipitates were further calcined at 550 ºC for 2 hrs. After calcination the powder were ground in an agate mortar. Particle size analysis displayed that almost 55% of the particles were smaller than 100 nm as shown in Figure 53 (The top figure is obtained from sedigraph and represents the cumulative particle size distribution. The bottom figure is obtained by Zetasizer and represents the distribution of the particle below 100nm (55w % of the powder)), and the mean particle size of the fraction below that point is about 90nm.

In order to investigate the relationship between the amount of reinforcement phase and related physical properties, 0,10,20 and 30vol% whisker containing HA composites were prepared.

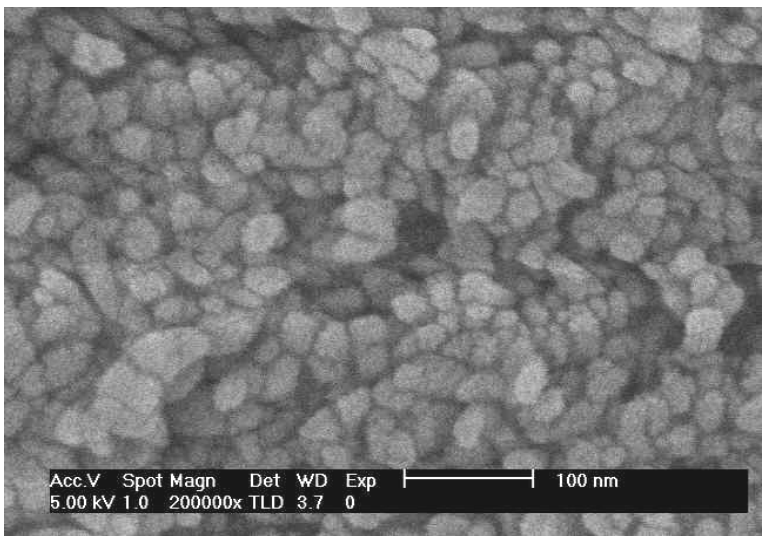

Figure 51. SEM micrograph of the powder precipitated at pH10 at 60 ^{o}C for 24h

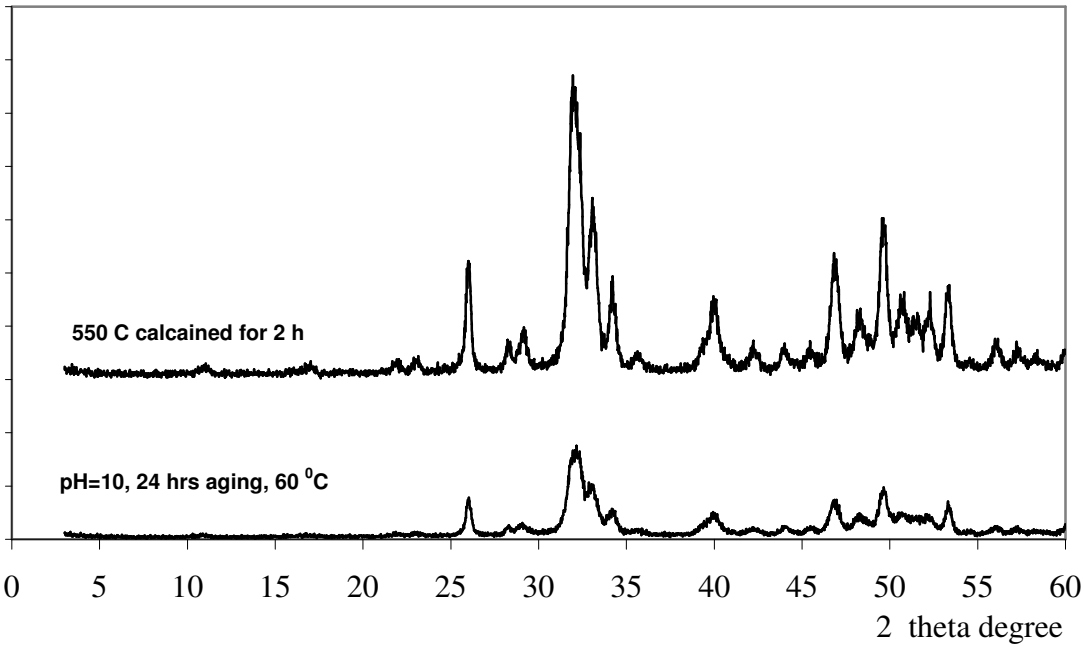

Figure 52. XRD pattrens of the precipitated powder at 60 °C and pH10 and after heat treatment at 550 °C.

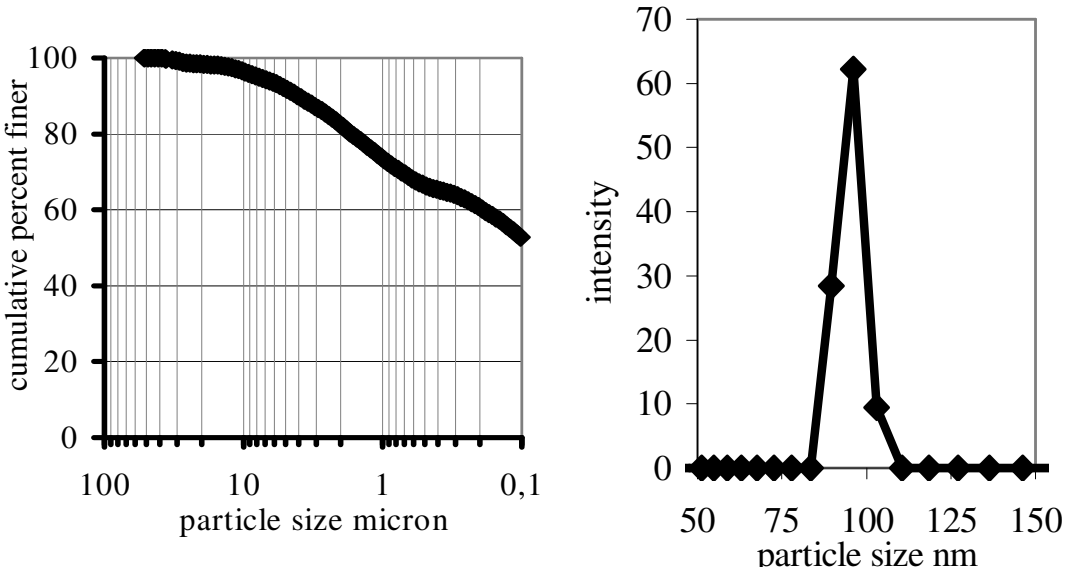

Figure 53. Particle size distribution of the powder precipitated at pH10 at 60 °C for 24h and after heat treatment at 550 °C.

6.2.1. Sintering Study

Dilatometric analysis was performed with similar regimes on the commercial and synthesized HA powder compacts in order to compare the densification behavior of these two powders. Linear shrinkage curves indicate that densification starts at 800 ºC and almost ends at 1250 ºC for both powders as seen in Figure 54. Density evolution data derived from shrinkage curves and further plotted in Figure 55 indicated that synthesized HA powder (DHA) experienced a higher densification up to 1250 ºC compared with the commercial powder. This result indicates that, unlike commercial powder, synthesized powder can be densified to full density in the 1000-1050 ºC range, as further implied by the extent of microstructure development seen in Figure 59 at 1000 ºC, by the manipulation of the sintering regime since dilatometric analysis were performed with 10 ºC / min heating rate. Conventional sintering studies performed under air atmosphere with 4 ºC/min heating rate and 2 hrs dwell time displayed that there is only 1-2 % density differences in the 1150-1300 ºC range sintered commercial HA powder compacts. Densification almost stops and 96-98 %TD was achieved in that range as seen in Figure 57. Open and closed porosity variation curves with temperature reveal that almost full densification can be achieved at 1100 ºC for commercial powder. As seen in Figure 58 open porosity disappeared at 1100 ºC and only 6-7 % closed porosity remains. Commercial and synthesized powder compacts both reached to the same density value of ~99 %TD at 1250 ºC and relatively large grains were observed in the microstructure compared to the initial powder particle sizes as seen in Figures 54, 55 and 57. This exaggerated grain growth seen in Figure 56 may deteriorate the mechanical properties.

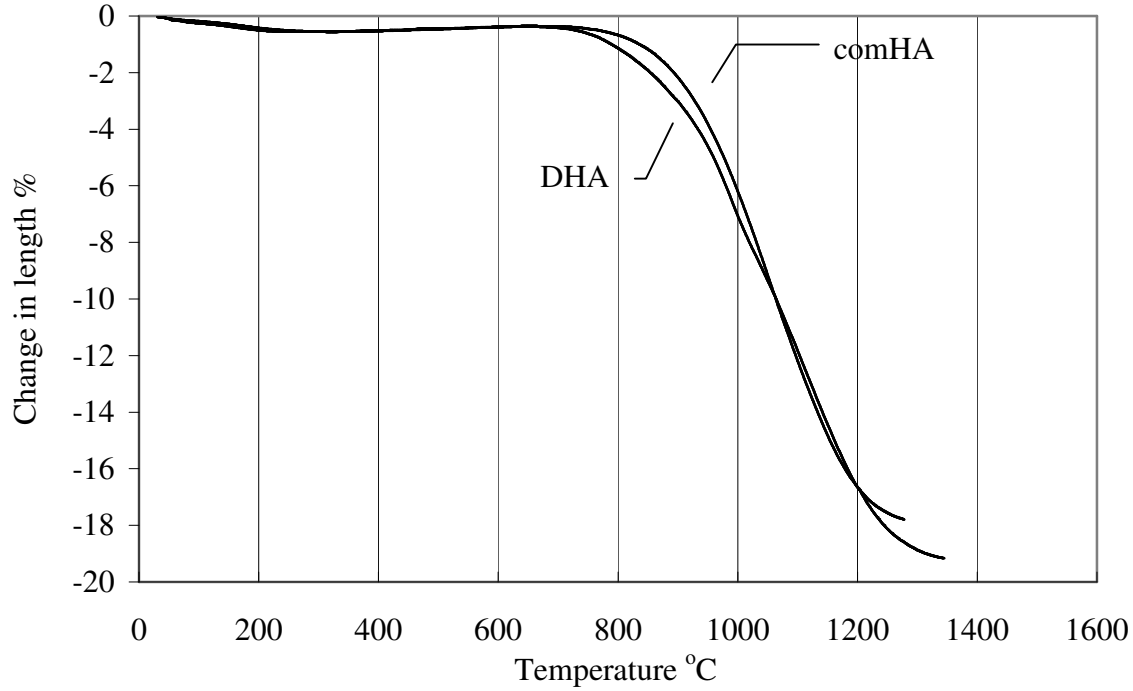

Figure 54. Dilatometric curves of the commercial and synthesized HA powder compacts.

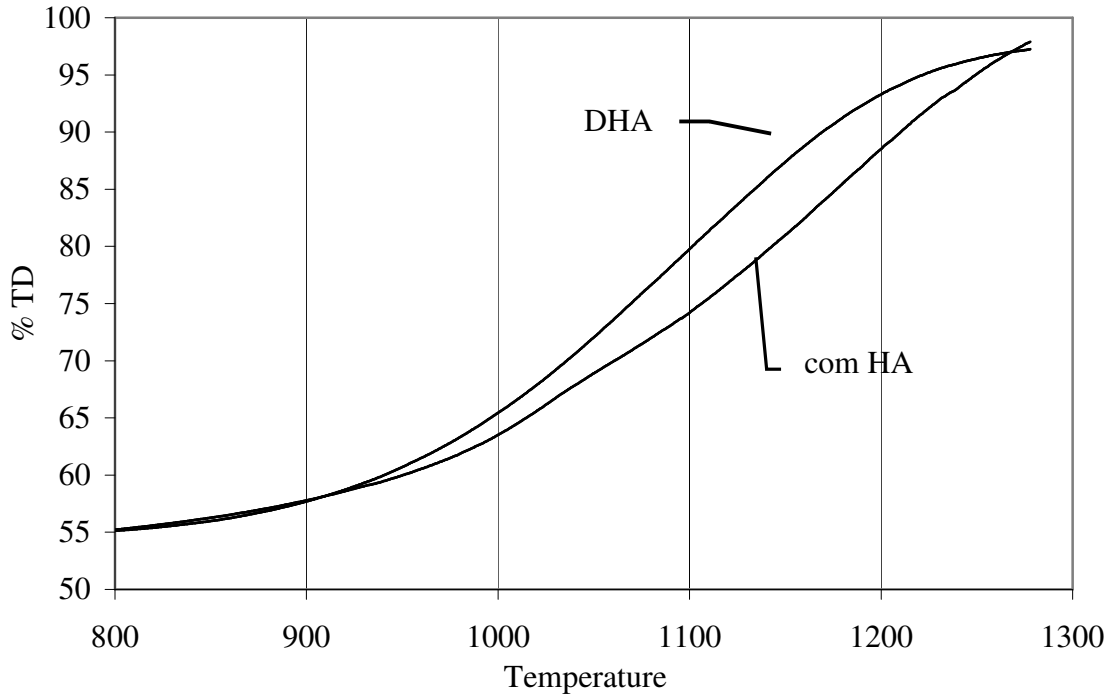

Figure 55. Densification behavior of the commercial and synthesized HA powders calculated from linear shrinkage curves.

Addition of reinforcement phase into the matrix led to a decrease in density as shown in Figure 57. Increase in the MSS type whisker content decreases the density of the composites and the highest density of 90 %TD was obtained from 10 vol% whisker containing composites at 1300 ºC. MSS whisker containing composites had different densities at 1300 ºC where as HDT type composites reached to a similar density value of ~95 %TD as seen in Figure 61 which may be explained by the decomposition of HDT whiskers into a TCP phase. On the other hand MSS whiskers are stable over 1300 ºC (32) and randomly oriented whisker network and pore structure formed during mixing, cannot be eliminated by sintering and led to formation of composites with relatively low final densities. Use of other compaction methods like extrusion, slip-casting that may align the whiskers in the green structure can enhance the densification behavior of the composites.

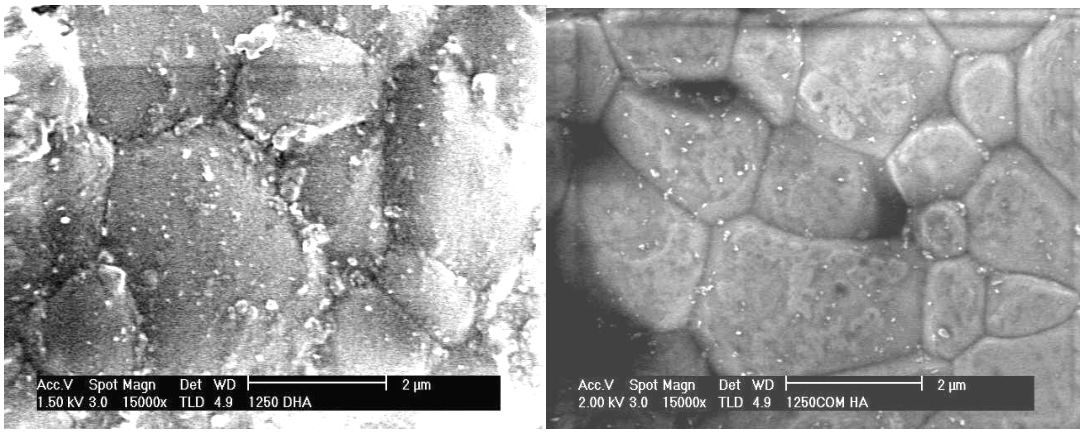

Figure 56. SEM micrographs of the synthesized and commercial HA ceramics sintered at 1250^0C

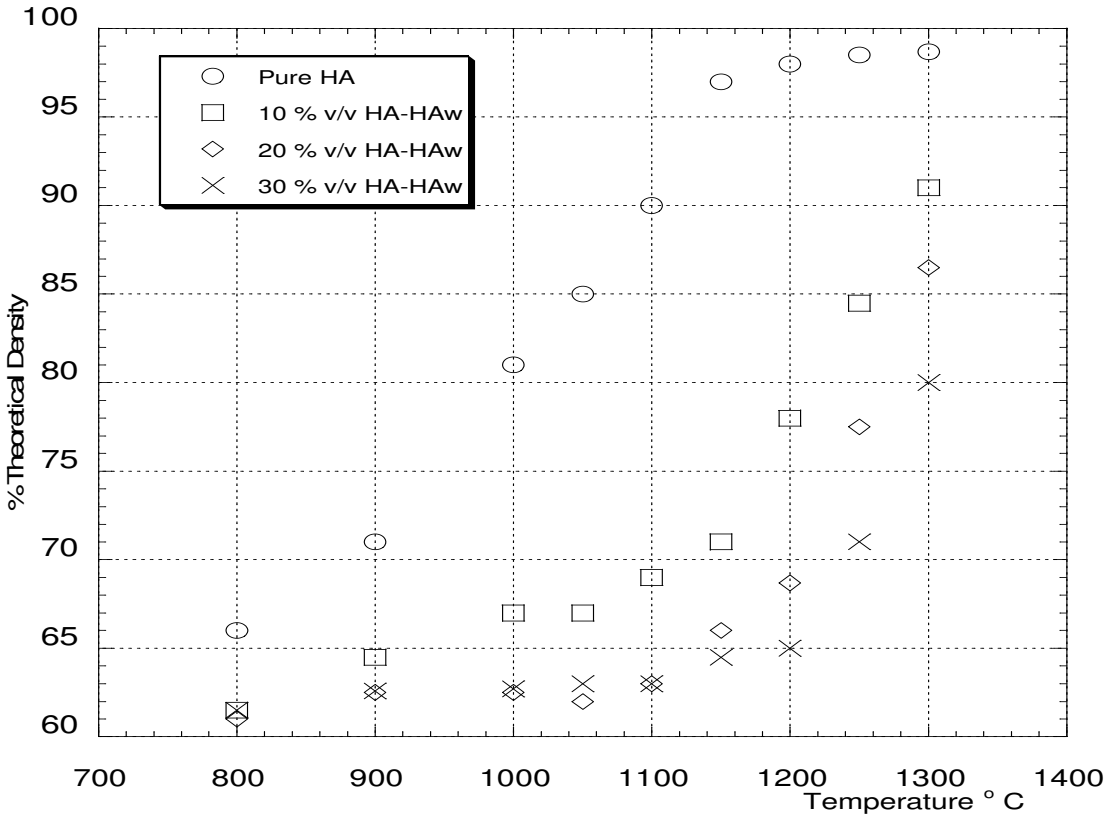

Figure 57. Sintering curves of pure commercial HA and MSS whisker containing composites

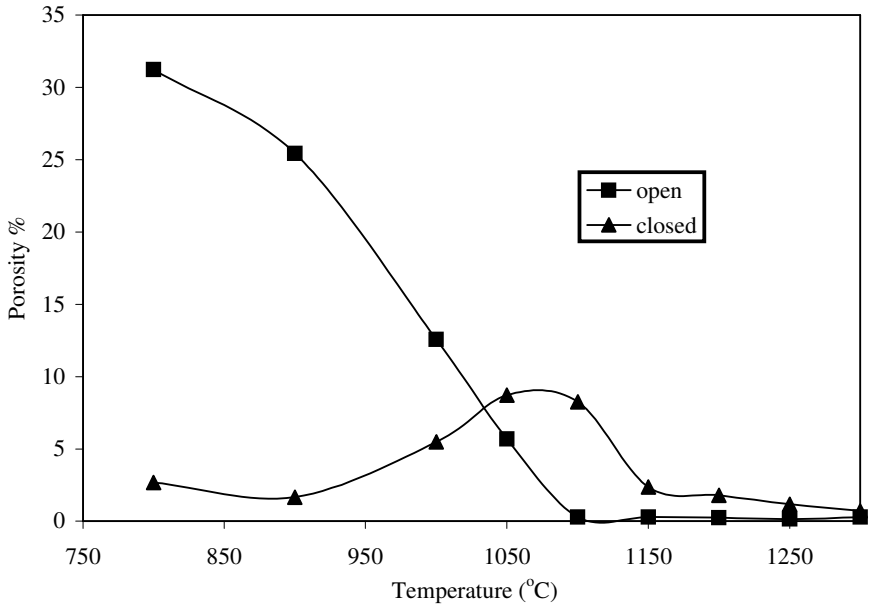

Figure 58. Change in open and closed porosity with respect to sintering temperature for pure commercial HA ceramics.

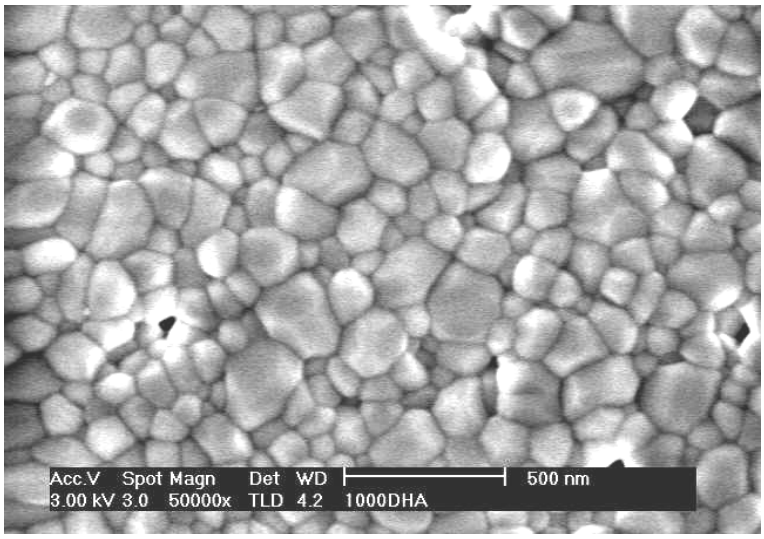

Figure 59. SEM micrograph of the synthesised HA ceramic sintred at 1000^0C

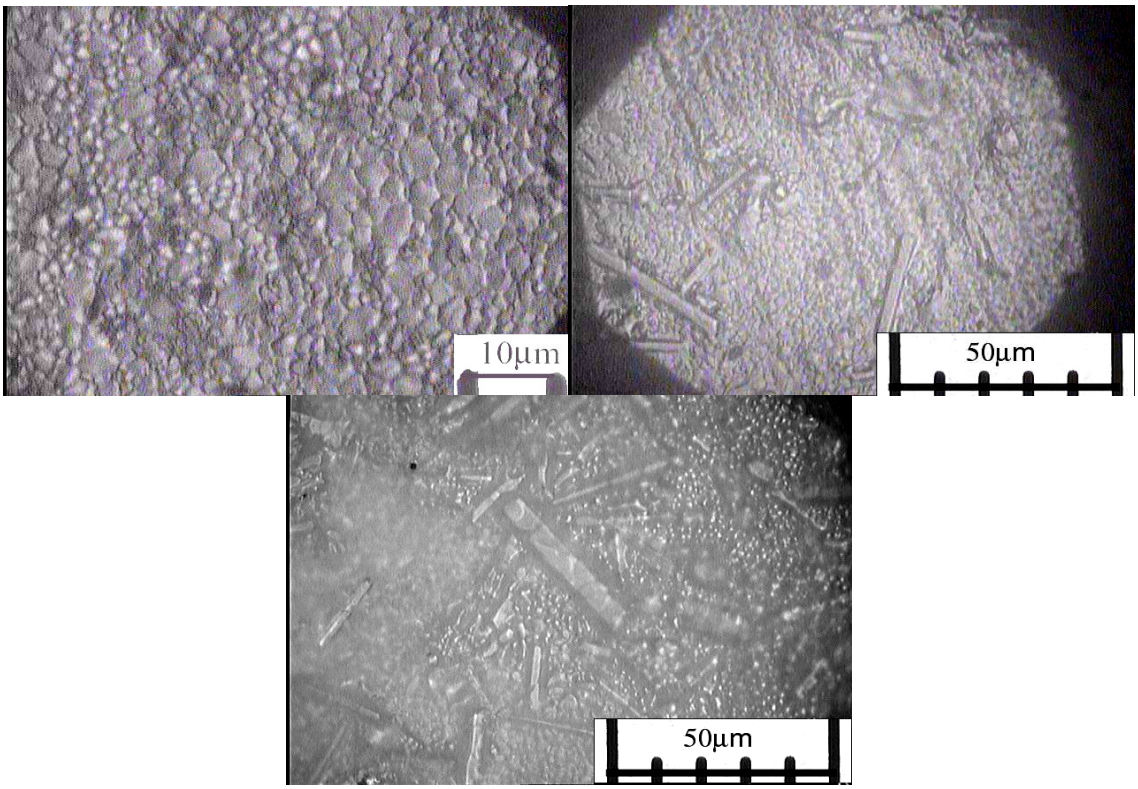

Figure 60. Optical microscopy micrographs ofthe commercial HA and MSS composites a) pure comHA b) 10%MSS+comHA composite c) 30% MSS+comHA composite

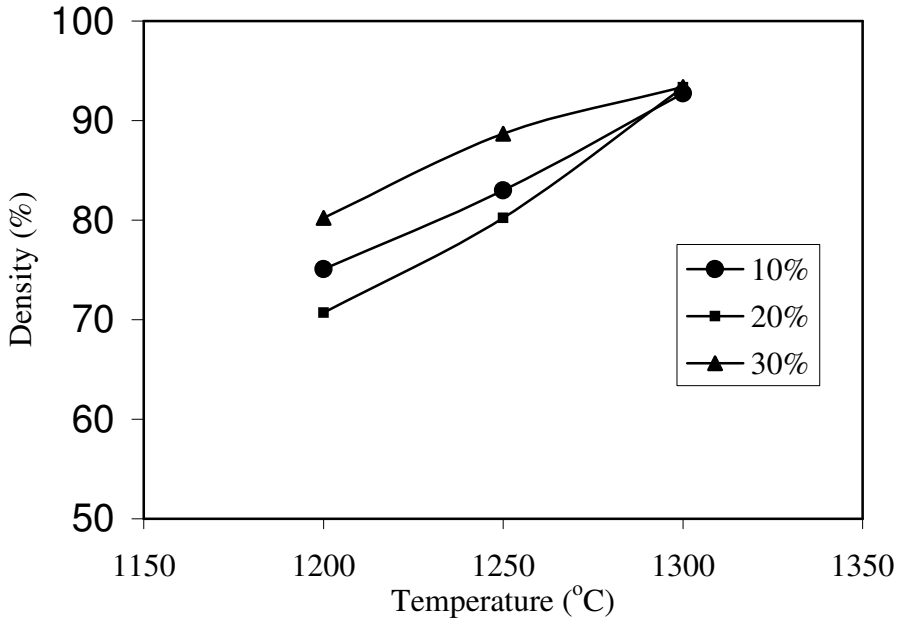

Figure 61. Densification behavior of commercial HA powder and hydrothermally synthesized whisker containing composites.

6.2.2. Mechanical Properties

HA composites with HA whiskers were prepared in order to improve the mechanical properties of pure HA ceramics without deteriorating biocompatibility. Mismatch in the mechanical properties may cause the stress concentration in the bone – implant interface under loading that may consequently end up with the death of surrounding tissue. Bone must be under a certain amount of load in order to remain healthy. If the bone is unloaded or over loaded in compression that leads to weakening of the bone and / or degradation of bone-implant interface.

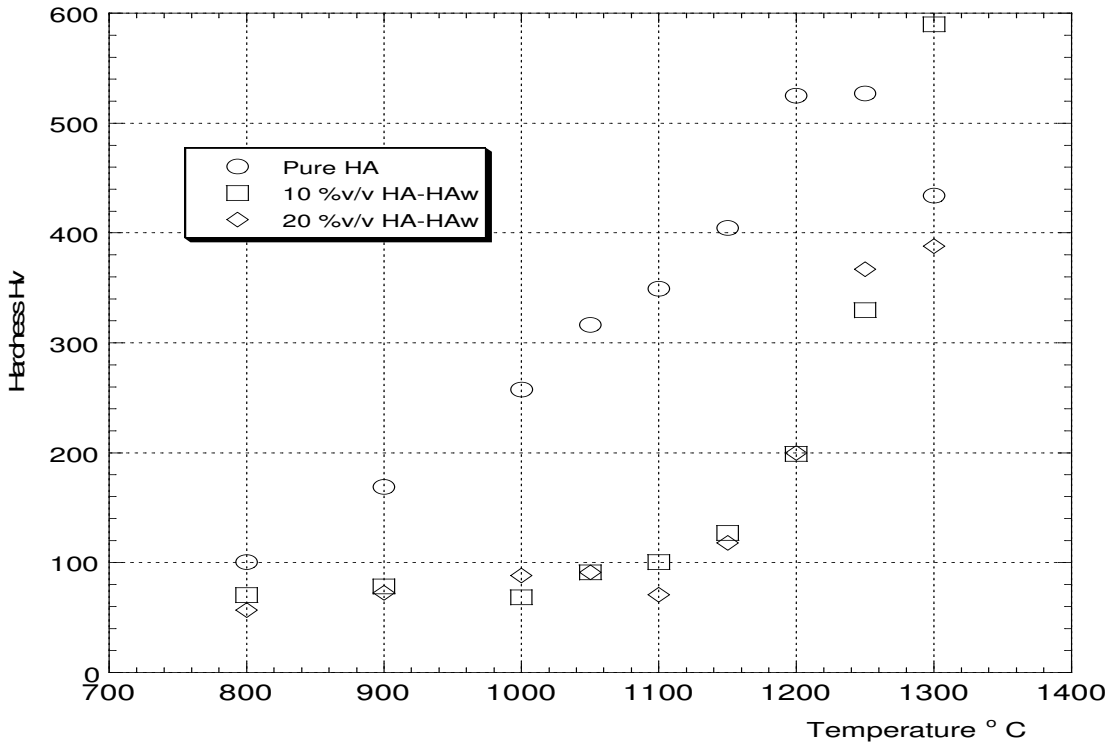

Figure 62. The change of the hardness of pure and MSS composite HA with the sintering temperature.

A continuous increase in hardness value of composites shown in Figure 62 is related with the increase in density with temperature. Commercial HA ceramics is also displays the similar behavior up to 1250 ^{o}C, but the decrease in hardness value at 1300 ^{o}C is related with the exaggerated grain growth and or partial decomposition of HA to TCP phase. The highest hardness value of ~580 Hv was obtained from 10vol% MSS whisker containing composites sintered at 1300 ºC with ~91%TD, on the other hand, ~91%TD was achieved at 1100 ºC for commercial HA ceramics had ~350 Hv hardness value.

Both commercial and synthesized HA ceramics displayed characteristic brittle fracture surfaces as seen in Figure 63. Addition of HA whiskers provide mechanical improvement by lengthen the crack path called as pullout mechanism as seen in from the SEM micrographs given Figures 64, 65 and 66. Whiskers in microstructure behave as a strong obstacle and increase the energy needed for the failure of material that leads to increase in strength as shown in compression testing results given in Figure 68.

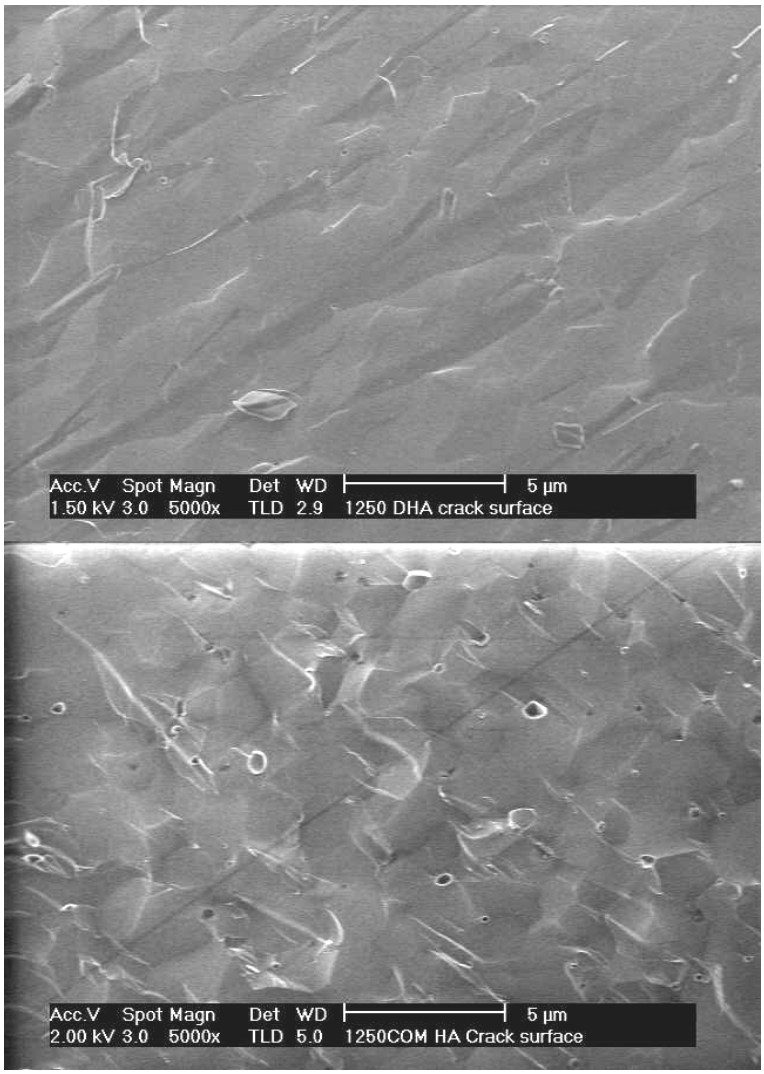

Figure 63. Fracture surfaces of synthesized and commercial HA ceramics sintered at 1250^0C

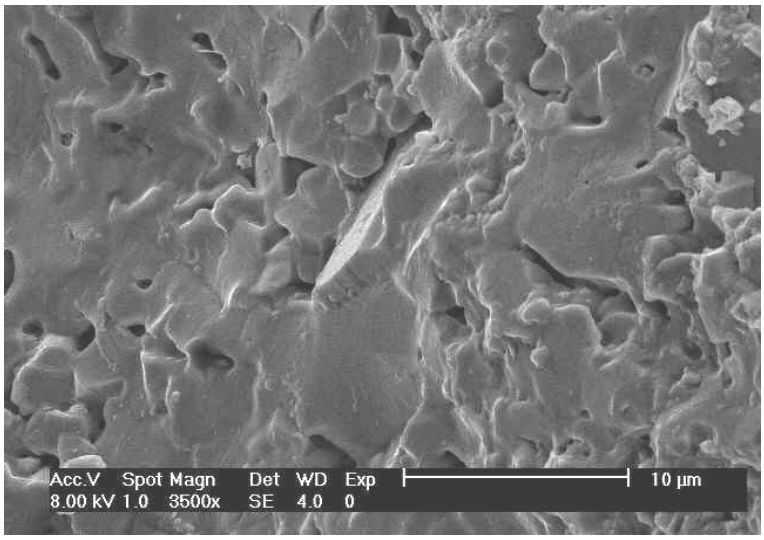

Figure 64. Fracture surface of 30vol% MSS containing commercial HA composites sintered at 1300^0C

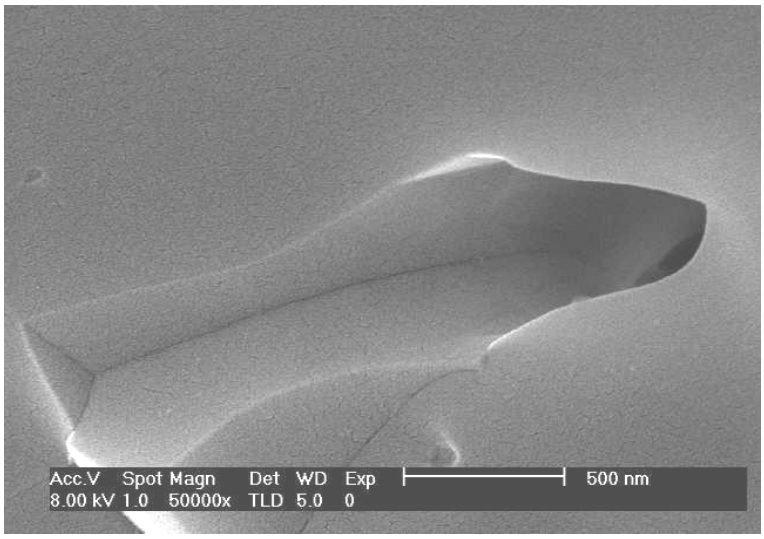

Figure 65. Fracture surface of 10vol% hydrothermally synthesized whisker containing commercial HA composites sintered at 1300^0C. Showing pullout.

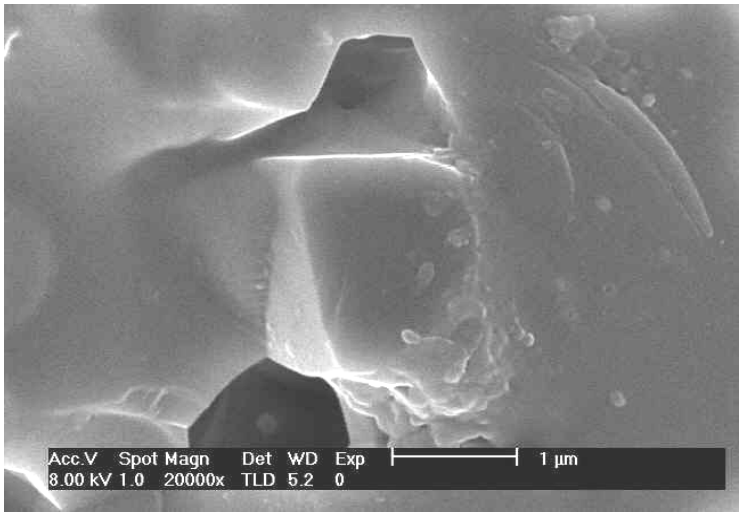

Figure 66. SEM micrograph display the pullout of whiskers at fracture surface of 10vol% hydrothermally synthesized whisker containing commercial HA composites sintered at 1300^0C.

Compressive strength result of the tested samples was significantly influenced by the compressive displacement of testing machine materials under loading as shown in Figure 67. The machine was loaded without sample and deflection amount was subtracted from the deflection of sample under same loading. Figure 68 displays the variation of compressive strength of commercial HA, 10,20 and 30 vol% MSS whisker

containing composites. As seen from the figure there was no significant difference in the compressive strength values of composites. On the other hand almost two-fold increase was achieved in the compressive strength values (460-470 MPa) with the addition of whiskers compared to that of commercial HA ceramic (240 MPa). Addition of whiskers was also increased the energy absorption capacity of HA ceramics that led to increase in strain at failure as shown in Figure 68. Compression testing results showed that at least 10vol% MSS whisker addition yields comparable compressive strength (460-470 MPa) and elastic modulus values (14-17 GPa) with that of natural bone tissues (170-193 MPa compressive strength, 14-18 GPa elastic modulus).

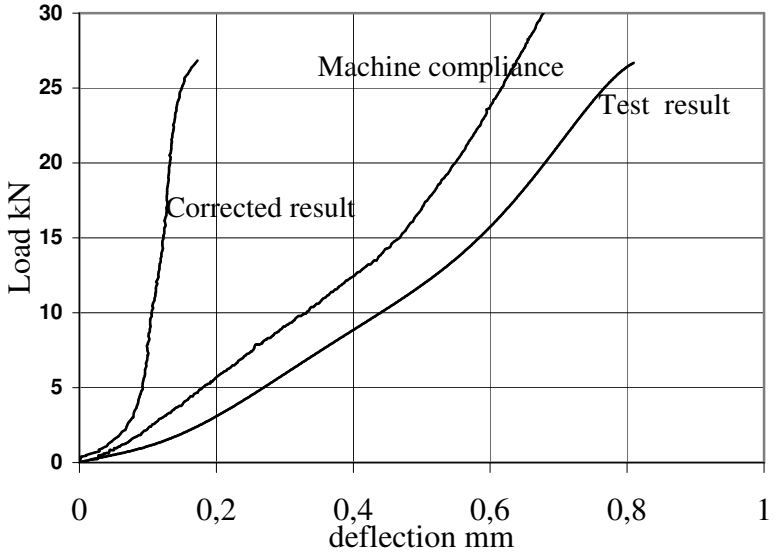

Figure 67. Load deflection graph of the pure commercial HA ceramic sintered at 1300^0C.Displays the effect of machine factor during compression.

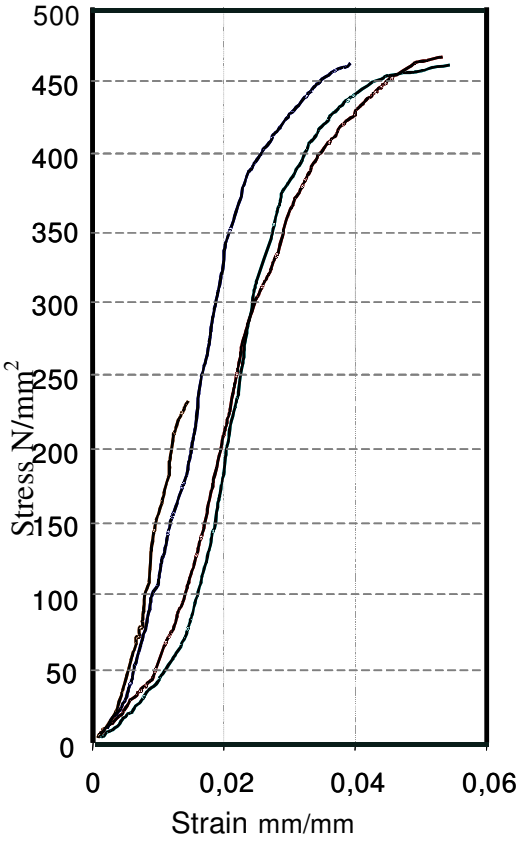

Figure 68. Load deflection graph of the pure commercial HA ceramic and 10, 20 30 vol % MSS whisker containing composites sintered at 1300^0C.

CHAPTER VII

CONCLUSIONS AND RECOMMENDATIONS

In this study the preparation and characterization of Ca-P powders, HA ceramics and composites have been investigated. Ca-P powders have been prepared by precipitation method by using aqueous solutions $(NH_4)_2HPO_4$ and $Ca(NO_3)_2$. $4H_2O$. Parameters of the precipitation conditions like pH aging time and temperature have been studied in detailed. Precipitates obtained from different conditions were characterized by several techniques like SEM, XRD, optical microscopy, sedigraph etc. Phase stability of the Ca-P powders was investigated at different temperatures by heat treatment at 400-1250 ^oC range. Optimum precipitation conditions for the synthesis of thermally stable HA powders were determined as pH=10, 60^oC aging temperature and 24hrs aging time. Precipitation conditions have significant effect on the Ca/P ratio of the synthesized powders. Further ICP and UV-Vis analyses are recommended for the control and determination of Ca/P ratio in the powder and sintered ceramics.

The sintering studies have shown that it is possible to prepare dense HA ceramics in the 1150-1250 ^oC range by synthesized powder. More detailed sintering studies along with in depth mechanical testing and fracture toughness analyses would give a better understanding of the densification behavior of these ceramics in this temperature range.

Two types of HA whiskers were prepared by MSS and HDT methods. Both whiskers displays very crystalline HA structures. HA composites with different whisker content were prepared and sintering behavior and mechanical properties investigated. Increase in the whisker content was decreased densities of composites sintered at different temperature. Use of other compaction methods like extrusion, slip casting may align the whiskers in the green structure that enhance the densification behavior of the composites. Comparable compressive strength and elastic modulus values with natural bone tissues were achieved by the usage of MSS HA whisker as a reinforcement phase. Detailed mechanical testing is recommended for the evaluation of fracture toughness of the HA ceramics and composites.

REFERENCES

1. Hench. L.L., “Bioceramics”, J.Am.Cer.Soc., 81(7)pp:1705-1728, (1998)
2. SuchanekW. and Yoshimura M. “ Processing and properties of HA based biomaterials for use as hard tissue replacement implants”, J.Mater. Res.,13(1)pp:94-116,(1998)
3. Hench L.L.,Wilson J., “bioceramics”, MRS Bulletinpp 62-74, September,(1991)
4. Pilliar R.M., Davies J.E. and Smith D.C, “ The bone- biomaterial interface for load-bearing implants”, MRS Bulletinpp 55-61, September,(1991)
5. Helmus M.N. “Overview of biomedical materials” MRS Bulletin pp 33-38, September,(1991)
6. Hench L.L” Medical materials for the next millennium”, MRS Bulletin,pp:13-19, May (1999)
7. Oonishi H. “Orthopaedic applications of HA”, Biomaterials, 171-178, 12, (1991)
8. www.saglık.gov.tr
9. Hench.L.L, Wilson J. “ An Introduction to Bioceramics” Advanced Series in Ceramics-Vol.1, World Scientific Publishing.,(1993)
10. Piconi C. and Maccauro G. “ Zirconia as ceramic biomaterial”, Biomaterials 20pp:1-25 (1999)
11. Gibson L.J. “ The mechanical behaviour of cancellous bone”, J.Biomechanics, 18(5),pp:317-328, (1985)
12. Corbridge D.E.C., “Phosphorous an Outline of its Chemistry, Biochemistry and Technology” Studies in Inorganic Chemistry 10, Elsevier,(1990)
13. Raynaud S., Champion E. Bernasche- Assollant D. Thomas P. “Calcium phosphate apatites with variable Ca/P atamic ratio I. Synthesiss, characterization and thermal stability of powders” Biomaterials, (2)pp:1065-1072,(2002)
14. Arends J., Christoffersen J., Christoffersen M.R., “A calcium HA precipitated from an aqueous solution” J. of Crystal Growth, 84, pp:515-532, (1987)
15. Royer A., Viguie J.C., “Stoichiometry of HA: influence on the flextural strength” J of Mat. Sci.: Material in Medicine, 4,pp:76-82,(1993)
16. Brown P.W., “ Phase relationship in the ternary system $CaO-P_2O_5-H_2O$ at 25^0C”, J.Am.Cer.Soc.75(1).,pp:17-22,(1992)

17. Suchanek W. Yashima M. Kakihana M. Yoshimura M. “ HA/ HA whisker composites without sintering additives: mechanical properties and microstructural evolution”, J.Am.Cer.Soc. 80(11),pp:2805-2813,(1997)
18. Lorenzo L.M.R. and Regi M.V. “ Controlled crystallization of calcium phosphate apatites” Chem.Mater.12 pp:2460-2465,(2000)
19. Lorenzo L.M.R. and Regi M.V., Ferreira J.M.F. “Fabrication of HA bodies by uniaxial pressing from a precipitated powder” Biomaterials, 22 pp:583-588, (2001)
20. Liu C., Huang Y., Shen W., Cui J. “kinetics of HA precipitation at pH 10-11” Biomaterials, 22 pp:301-306, (2001)
21. Guicciardi S. Galassi C. Landi E. “ Rheological characteristics of slurry controlling the microstructure and the compressive strength behaviour of biomimetic HA” J.Mater.Res.,pp: 16(1),163-170(2001)
22. Ahn E. Gleason N.J. Nakahira A., Ying J.Y. “Nanostructure processing of HA based bioceramics”, Nano Let.1(3),pp:149-153, (2001)
23. Hattori T., İwadate Y., Kato T. “ Hydrothermal synhthesis of HA from calcium pyrophosphate""J.Mater.Sci.Let. 8. Pp: 305-306 (1989)
24. Nagata F.,Yakogawa Y., Toriyama M. “ Hydrothermal synthesis of platelike HA crystals” Advanced Materials 1993,II/A: Biomaterials, Organic and İntelligent Materails, Edited by H.Aoki et al. Trans. Mat.Res.Soc. Jpn., vol 15A 1994,
25. Yoshimura M., Suda H. Okamoto K., İoku K. “ Hydrothermal synthesis of biocompatible whiskers” J. of Mater.Sci. 29 pp: 3399-3402, (1994)
26. Suchanek W., Suda H., Yashima M., Kakihana M., Yoshimura M. “ biocompatible whiskers with controlled morphology and stoichiometry” J.Mater. Res. 10(3),pp:521-529(1995)
27. Fujishiro Y., Yabuki H., Kawamura K., Sato T., Okuwaki A., “Preparation of needle-like HA by homogeneous precipitation under hydrothermal conditions”, J. Chem. Tech. Biotechnol. 57 pp:349-353 (1993)
28. Ioku K., Yoshimura m., Somia S., “Microstructure and mechanical propertirs of HA ceramics with zirconia dispersion prepared by post-sintering”, Biometarials 11,pp:57-61 (1990).
29. Monma H., Ueno S., Kanazawa T., “ Prpperties of HA prepared by the hydrolysis of tricalcium phosphate”, J. Chem. Tech. Biotechnol. 31 pp:15-24 (1981)
30. Monma H., Kamiya T., “Preparation of HA by the hydrolysis of brushite”, J. Mater. Sci., 220, pp:4247-4250 (1987).

31. Yubao L., Xingdong Z., De Groot K., "Hydrolysis of phase transition of alpha-tricalcium phosphate", Biomaterials 18 pp:737-741 (1997).
32. Taş C.A., "Molten salt synthesis of calcium HA Whiskers", J. Am. Ceram. Soc. 84 (2), pp:295-300 (2001)
33. Shirekhanzadeh M., Azadegan M., " HA particles prepared by electro crystallization from aqueous electrolytes", Mat. Let. 15 pp:392-395 (1993).
34. Verbeeck R. M. H., de Maeyer E.A. P., Driessens F. C. M., " Stiochiometri of potassium and carbonate containing apatites synthesised by solid state reactions", Inorg. Chem. 34 pp: 2084-2088 (1995).
35. Fulmer M. T., Brown P. W., "Effects of temperature on the formation of HA", J. Mater. Res. 8(7), pp:1687-1696 819939.
36. Arita I. H., Castano V. M. Wilkinson D. S. "Synthesis osn processing of HA ceramic tapes with controlled porosity", J. of Mat. Sci. : Materials in Medicine 6 pp:19-23 (1995).
37. Raynaud S., Champion E. Bernasche- Assollant D. Thomas P. "Calcium phosphate apatites with variable Ca/P atamic ratio III.Mechanical properties and degradation in solution of hot pressed ceramics" Biomaterials, 23 pp:1081-1089,(2002).
38. Raynaud S., Champion E. Bernasche- Assollant D. Thomas P. "Calcium phosphate apatites with variable Ca/P atamic ratio II.Calcination and sintering" Biomaterials, 23, pp:1073-1080,(2002).
39. Landuyt P. V., Li F., Keustermans J. P., Streydio J. M., Delannay F., "Yhe influence of high sintering temperatures on the machanical properties of HA", J. of Mat. Sci. : Materials in Medicine ,6, pp:8-13 (1995).
40. Ramachandra Rao R., Kannan T.S., " Dispersion and slip casting of HA", J. Am. Ceram. Soc., 84 (8), pp: 1710-1716 (2001).
41. Liu D.M. " Praparation and characterization of porous HA bioceramic via a slip-casting route", Ceramics Int.24 pp:441-446 (1998).
42. Lim G. K., Wan J., Ng S.C., Chew C. H., Gan L. M., "Pracessing of HA via microemulsion and emulsion routes", Biomaterials 18, pp:1433-1439 (1997).
43. Layrolle P., Ito A., Tateishi T., "Sol-gel synthesis of amorphous calcium phosphate and sintering into microporous HA bioceramics", J. Am. Ceram. Soc., 81 (6), pp: 1421-1428 (1998).

44. Deptula A., Lada W., Olczak T., Borello A., Allani C., di Bartolemeo A., "Preparation of spherical powders of HA by sol-gel process", J. of Non Crystalline Solids 147 & 148 pp:537-541 (1992).
45. De With G., Corbijn A. J., "Metal fibre reinforced HA ceramics", J. of Mat. Sci., 24 pp:3411-3415 (1989).
46. Knepper M., Moricca S., Milthorpe B. K., " Stability of HA while processing short-fibre reinforced HA ceramics", Biomaterials 18, pp:1523-1529 (1997).
47. Li J., Liao H., Hermansson L., "Sintering of partially-stabilized zirconia and partially-stabilized zirconia-HA composites by hot-isostatic pressing and pressureless sintering", Biomaterials 17, pp:1787-1790 (1996).
48. Silva V. V., Lamerias F. S., Domingues R. Z., "Microstructural and mechanical study of zirconia-HA composite ceramics for biomedical applications", Composites Sci. and Tech. 61, pp:301-310 (2001)
49. Silva V. V., Lamerias F. S., " Synthesis and characterization of composite powders of partially stabilized zirconia and HA", Materials Characterization 45 pp:51-59 (2000).
50. Suchanek W., Yashima M., Kakihana M., Yoshimura M., " Processing and mechanical properties of HA reinforced with HA whiskers", Biomaterials 17, pp:1715-1723 (1996).
51. Ruys A. J., Wei M., Sorrell C.C., Dickson M. R., Brandwood A., Milthorpe B. K., " Sintering effects on the strength of HA", Biomaterials 16, pp:409-415 (1995).
52. De With G., Vandijk H. J. A., Hattu N., Prijs K., " Preparation, microstructure and mechanical properties of dense polycrystalline HA", j. Mater. Sci., 16 pp:1592-1598 (1981).
53. Gautier S., Champion E., Bernache-Assolant D., Chartier T., "Rheological characteristics of alumina platelet-HA composite suspensions", J. Euro. Ceram. Soc., 19, pp:469-477 (1999).